DEPARTMENT OF THE ARMY CORPS OF ENGINEERS, U. S. ARMY

BEACH EROSION BOARD
OFFICE OF THE CHIEF OF ENGINEERS

AN EXPERIMENTAL STUDY OF SUBMARINE SAND BARS

TECHNICAL REPORT NO. 3

AN EXPERIMENTAL STUDY OF SUBMARINE SAND BARS

TECHNICAL REPORT NO. 3

BEACH EROSION BOARD
OFFICE OF THE CHIEF OF ENGINEERS

DEPARTMENT OF THE ARMY

OFFICE OF THE CHIEF OF ENGINEERS

BEACH EROSION BOARD

The Beach Erosion Board of the Department of the Army was established by section 2 of the River and Harbor Act approved 3 July 1930 (Public, 520, 71st Cong.), to cause investigations and studies to be made in cooperation with the appropriate agencies of various States on the Atlantic, Pacific, and Gulf coasts, and on the Great Lakes, and the Territories, with a view to devising effective means of preventing erosion of the shores of the coastal and lake waters by waves and currents. The duties of the Board were modified by an act approved 31 July 1945 (Public, 166, 79th Cong.), "to make investigations with a view to preventing erosion of the shores of the United States by waves and currents and determining the most suitable methods for the protection, restoration, and development of beaches; and to publish from time to time such useful data and information concerning the protection of the beaches as the Board may deem to be of value to the people of the United States * * *."

TECHNICAL REPORTS

Technical Report No. 1—A Study of Progressive Oscillatory Waves in Water, 1941.

Technical Report No. 2—A Summary of the Theory of Oscillatory Waves, 1941.

Technical Report No. 3—An Experimental Study of Submarine Sand Bars, 1948.

August 1948.

This paper was prepared for the Beach Erosion Board during World War II by Dr. Garbis H. Keulegan of the Hydraulics Laboratory of the National Bureau of Standards. Dr. Keulegan completed work for this paper in 1944 while detailed to the Beach Erosion Board as a consultant in hydrodynamics. While this paper was prepared primarily for departmental use and the opinions and conclusions expressed are those of the author, it is believed that it will be of material value to engineering and research agencies engaged in work involving submarine sand bars.

CONTENTS

LIST OF ILLUSTRATIONS

LIST OF SYMBOLS

A = Cross-sectional area.
a = Measured wave height in front of wave generator.
a_o = Corresponding deep water wave height.
C = Crest of the submarine sand bar.
γ_s = Specific weight of sand.
D = Distance traveled by a sand ripple.
d_{GM} = Median diamteer of sand.
Δf_1 = Elevation of the wave crest above the undisturbed water surface.
Δf_2 = Depression of the wave trough below the undisturbed water surface.
ΔH_1 = Maximum elevation of the surface above the undisturbed water surface during the passage of waves.
ΔH_2 = Depression of the trough at the start of wave break.
H_1 = Undisturbed water depth.
H_2 = Depth of water at the point where wave reformation begins.
H_B = Depth from the undisturbed water surface to the bar base when the bar becomes relatively stable.
H'_B = Depth from the undisturbed water surface to the bar base when the bar is in the process of formation.
H_c = Depth of the bar crest below the undisturbed water surface.
H_t = Depth of the bar trough below the undisturbed water surface.
i = Slope of the beach.
λ = Measured wave length in front of the wave generator.
λ_0 = Corresponding deep water wave length.
ν = Kinematic viscosity.
0 = Reference point for measuring and identifying stations.
Q = Rate of sand transportation.
Q_r = Weight of sand transported per hour per foot of width.
P_s = Density of sand.
P_w = Density of water.
s = Distance between the point where the wave begins to break and the breaker is completed.
S_1 = Point of impending wave break.
σ_φ = Logarithmic standard deviation (Krumbein's notation).
T = Period of the wave.
t_1 = Time required for the bar to become relatively stable.
y = Depth of any point with respect to the undisturbed water surface.
z = Horizontal distance from a vertical line passing through the center of the crest of the bar to any other point at depth y.

LIST OF SYMBOLS

A = Cross-sectional area.

a = Measured wave height in front of wave generator.

a_o = Corresponding deep water wave height.

C = Crest of the submerging sand bar.

γ = Specific weight of sand.

D = Distance traversed by a sand dipple.

d_{50} = Median diameter of sand.

$\Delta\zeta$ = Elevation of the wave crest above the undisturbed water surface.

$\Delta\zeta_1$ = Depression of the wave trough below the undisturbed water surface.

$\Delta\zeta_2$ = Maximum elevation of the surface above the undisturbed water surface during the passage of waves.

$\Delta\zeta_3$ = Depression of the trough at the start of wave break.

H = Undisturbed water depth.

H_1 = Depth of water at the point where wave deformation begins.

H_2 = Depth from the undisturbed water surface to the bar crest when the bar becomes relatively stable.

H'_2 = Depth from the undisturbed water surface to the bar crest when the bar is in the process of formation.

H_3 = Depth of the bar crest below the undisturbed water surface.

H_4 = Depth of the bar trough below the undisturbed water surface.

i = Slope of the beach.

λ = Measured wave length in front of the wave generator.

λ_o = Corresponding deep water wave length.

μ = Kinematic viscosity.

θ = Reference point for measuring and identifying stations.

Q = Rate of sand transportation.

Q_s = Weight of sand transported per hour per foot of width.

ρ_s = Density of sand.

ρ_w = Density of water.

s = Distance between the point where the wave begins to break and the breaker is completed.

S_1 = Point of impending wave break.

σ_o = Lagrangian standard deviation (Cornubia's notation).

T = Period of the wave.

t = Time required for the bar to become relatively stable.

y = Depth of any point with respect to the undisturbed water surface.

z = Horizontal distance from a vertical line passing through the center of the crest of the bar to any other point at depth y.

AN EXPERIMENTAL STUDY OF SUBMARINE SAND BARS

Section I. INTRODUCTION

Submarine sand bars are frequently found as characteristic features of ocean and lake beaches. The bars may occur singly or in series and are usually associated with sand beaches and offshore areas. An individual bar formation consists of a crest or ridge to seaward and a trough or depression, to shoreward. A series of bars is a number of related crests and troughs. These bar formations have been studied by geographers and geologists, and the literature on the subject has a history of almost three quarters of a century. The earliest descriptions of these underwater formations were those of the German investigator Hagen, whose work appeared in 1863 (reference 1) and was followed by that of Otto, Lehmann, Hartnack, and Evans (references 2, 3, 4, and 5) among others. Although considerable data on the material aspects (form, dimensions, and number) of bars is thus available, almost no authoritative information on the mechanism of bar formation and movement has been obtained.

Admittedly the formation and migration of offshore sand bars are hydrodynamical phenomena of a complex nature difficult to study in a natural environment; under these circumstances laboratory experimentation can prove of considerable value. Economy of time, the limitations of available apparatus, and the nature of the problem require that the general case be resolved into components. Each component can then be considered individually as involving only a limited number of variables. The present investigation concerns, as a first step, the metrical aspects of bars; i. e., the shape and disposition of bars, as they are influenced by the size characteristics of waves.

This paper reports the results of experiments made to determine the existence of basic relationships governing bar phenomena. Observations were made of the form, dimensions, and number of bars; wave characteristics; ripple formation; and nature and volume of sand movement involved in bar phenomena. During the investigation certain qualitative observations on some of the factors affecting the mechanism of bar formation and movement were made. Although these qualitative observations are limited, they will be discussed briefly because of their implications for further study.

806229—48——2

Section II. PRELIMINARY CONSIDERATIONS

A. *Bar formation.*—If an experimental beach be assumed having initially a smooth sand surface of constant slope and subject to the action of waves, the part of the beach which lies between the point of impending wave break and that of reformation following the breaker is the area of most active change. This region may be called the bar environment since it is here that the bar is ultimately formed. As will be discussed more fully later, the breaker is the most important element of the region and is the genetic cause of the bar itself.

The deformation of the beach surface is in the form of a ridge, which is relatively flat in the initial stages and moves toward the shore in an observable manner. In the course of time the ridge is enlarged, its form is established or stabilized and its motion decreases to an imperceptible value. When the changes in the position and shape of the bar become minute, the bar can be considered relatively stable. Thus, beginning with an initial smooth beach of slope i at time $t=0$, the bar will reach a stable position and assume a stable shape at time t_1, such that after that time the changes in the bar position and the bar shape take place at an imperceptible rate. Hence, t_1 may be said to be the time required for the bar to become relatively stable. The first problem in studying bar formation therefore is to determine the factors which affect the position of the bar at the time that it becomes relatively stable.

The dimension defining the position of bars in a hydrodynamical sense must necessarily be selected. Inasmuch as the types of bars considered here are associated with breaking waves, the relevant dimension is the depth of the bar with respect to the undisturbed water surface rather than the distance between the bar and the shore. The depth of the bar can be represented by the bar base, defined as the straight line joining the seaward and shoreward toes of the bar (fig. 1.) The depth of the bar base is measured from the undisturbed water surface to the point directly below the crest, C. This depth will be denoted by H'_B when the bar is in the process of formation and by H_B after the bar becomes relatively stable.

Suppose that the variables affecting H'_B are the deep water wave length λ_0, wave height a_o, time t, the sand size d_{GM}, the sand size distribution coefficient σ_φ (Krumbein notation), the kinematic viscosity ν, the sand and water densities P_s and P_w, respectively, and the slope of beach i. The usual considerations of dimensional analysis then lead to the general relation:

$$f\left(\frac{a_o}{H'_B}, \frac{a_o}{\lambda_0}, \frac{d_{GM}\sqrt{ga_o}}{\nu}, \frac{\lambda_0}{d_{GM}}, \sigma_\varphi, i, \frac{P_s}{P_w}, \frac{T}{\sqrt{g\lambda_0}}\right)=0 \qquad (1)$$

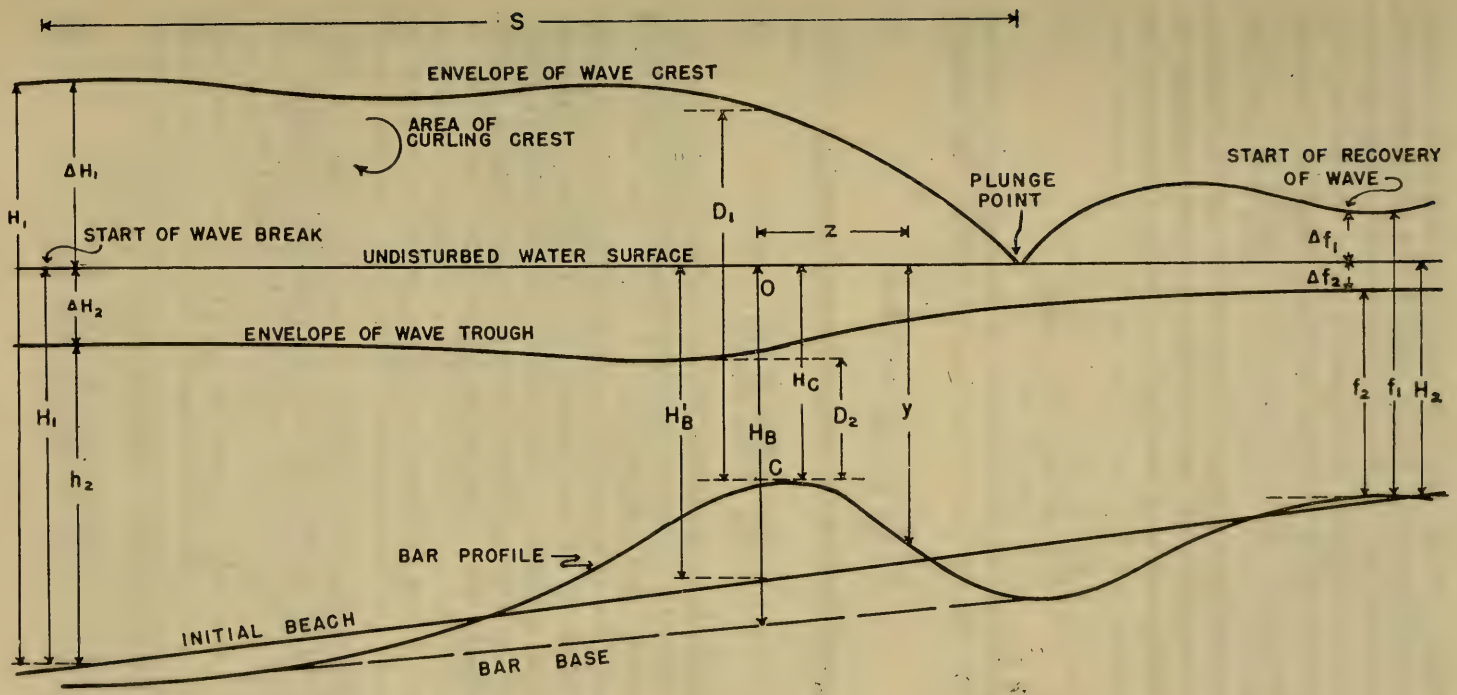

DEFINITIONS OF TERMS DESCRIBING THE BAR ENVIRONMENT

FIGURE 1.

The dimensionless terms are the transfer parameters relating phenomena of different scale. The multiplicity of these parameters makes the possibility of a true model experiment of bar processes questionable, if not negative. It is possible, however, that approximate models which ignore the least important terms are sufficient. The term, $\frac{P_s}{P_w}$, may be omitted because the densities are constant. If it is assumed that hydrodynamic effects on the motion of sand are independent of the Reynolds number, the parameter containing the kinematic viscosity also may be eliminated. With these simplifications,

$$f_1\left(\frac{a_o}{H'_B}, \frac{a_o}{\lambda_0}, \frac{\lambda_0}{d_{GM}}, \sigma_\varphi, i, \frac{T}{\sqrt{g\lambda_0}}\right)=0 \tag{2}$$

To obtain the equation for the bar after it is relatively stable, H_B may replace H'_B and the term involving time be omitted. Accordingly,

$$f_1\left(\frac{a_o}{H_B}, \frac{a_o}{\lambda_0}, \frac{\lambda_0}{d_{GM}}, \sigma_\varphi, i,\right)=0 \tag{3}$$

or omitting σ_φ, which may be a constant for a series of tests.

$$\frac{a_O}{H_B}=f_2\left(\frac{a_o}{\lambda_0}, \frac{\lambda_0}{d_{GM}}, i\right) \tag{4}$$

The last expression suggests that the effect of wave height, a_o, and the bar base depth H_B can be conveniently related by plotting a_o/H_B against the wave steepness ratio a_o/λ_0.

B. *Depth and form of bars.*—The depth of the bar crest below the water surface (H_c in fig. 1) is the highest point of the bar and therefore is probably a critical feature. It may then be assumed that a relationship exists between the bar depth, the wave characteristics and the nature of the sand. The general expression

$$f_2\left(\frac{H_c}{a_o}, \frac{a_o}{\lambda_0}, \frac{\lambda_0}{d_{GM}}, \sigma_\varphi, i\right)=0 \tag{5}$$

is obtained from dimensional analysis by assuming that the bar is relatively stable and the effect of kinematic viscosity is negligible. In view of equation 3, H_c/a_o may be replaced by H_c/H_B, giving

$$\frac{H_c}{H_B}=f_3\left(\frac{a_o}{\lambda_0}, \frac{\lambda_0}{d_{GM}}, \sigma_\varphi, i\right) \tag{6}$$

If $\sigma\varphi$ is the same in all tests it suffices to write

$$\frac{H_c}{H_B}=f_3\left(\frac{a_o}{\lambda_0}, \frac{\lambda_0}{d_{GM}}, i\right) \tag{7}$$

Accordingly the depth and form of the bar can be related to wave characteristics by considering the dependence of H_c/H_B upon a_o/λ_0.

A more complete description of a bar is obtained from an examination of variations in the form, considering the bar profile as the form. The general relation defining the bar profile is obtained as follows. Any point on the profile may be determined by the parameters y and z (see fig. 1) in which y is the depth of the point with respect to the undisturbed water surface and z is the horizontal distance from a vertical line passing through the crest, C, of the bar. This distance will be regarded as positive if the point is shoreward of C. By dimensional reasoning as in Equation 6, we obtain the relationship:

$$\frac{\gamma}{H_B}=f\left(\frac{z}{H_B}, \frac{a_o}{\lambda_0}, \frac{\lambda_0}{d_{GM}}, \sigma_\varphi, i\right) \tag{8}$$

and again neglecting σ_φ,

$$\frac{\gamma}{H_B}=f\left(\frac{z}{H_B}, \frac{a_o}{\lambda_0}, \frac{\lambda_0}{d_{GM}}, i\right) \tag{9}$$

which is the desired general relation for the form or configuration of bars.

Section III. EQUIPMENT AND PROCEDURE

Experiments were made in two wave tanks, one 1.5 feet wide, 2 feet deep and 30 feet long; the other 14 feet wide, 4 feet deep and 85 feet long. Schematic views of the small and large tanks are shown in figure 2A and 1B, respectively. The conditions illustrated are those for a beach having a slope of 1 on 70. The experimental beach for each sketch is to the left of the mark *0;* the section to the right of the mark is a transition. In a more suitable tank this transition section would not have been necessary; instead the beach slope would have extended to the bottom. The distorted proportions of the approach, or transition segment, restrict the normal motion of the sand toward the experimental beach and thus might alter the dimensions of the bar eventually formed. It is considered that the test results for the 1/70 slope may be affected by these conditions but those for the steeper slopes are believed to be reliable. The mark *0* of the figure is solely a reference point for measuring distances and identifying stations. The depth of water in front of the wave generator is variable, the depth being adjusted, depending on the height of the waves, to control the position of the breaking waves on the experimental beach.

Tests in the small tank were made with beach slopes of 1 on 70, 1 on 30, and 1 on 15. Those slopes were established always to the left of *0*, with the transition segment to the right of *0* the same for all

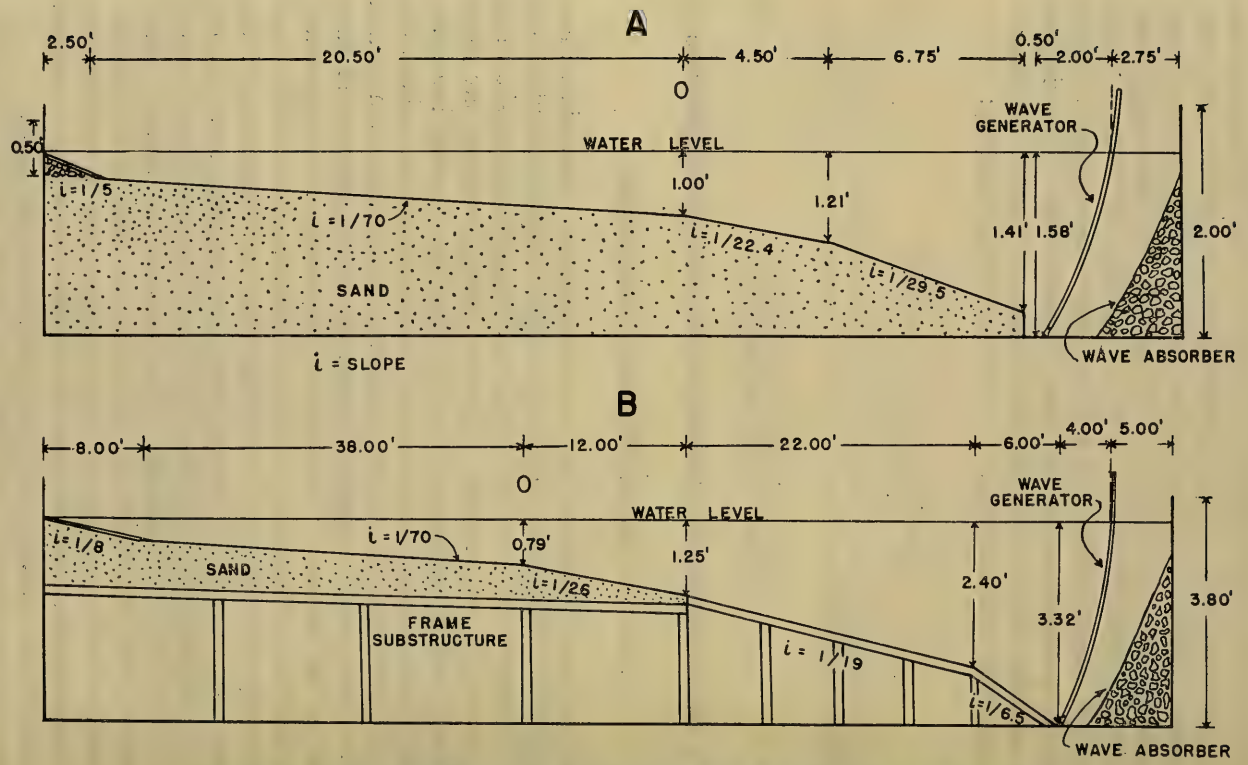

SCHEMATIC VIEWS OF BEACH AND WAVE APPARATUS

FIGURE 2.

three slopes. The small tank is provided with a glass wall allowing observation of the experimental beach.

The large tank was subdivided into three parallel compartments with beach slopes of 1 on 30, 1 on 50, and 1 on 70, respectively. The experimental beach of slope 1 on 70 is shown in figure 2B. The sand of the experimental beach and of a part of the approach segment is placed on a platform. The remaining major part of the approach segment, consisting of a wooden platform, is firmly attached to the concrete bottom of the tank. In the sketch the experimental beach is to the left of mark *0*, and the approach segment of the right of *0*. In the three compartments the approach conditions were alike.

The sand used for the experiments was commercial Potomac River sand. Sieve analysis for the distribution of grain size gave the following percentage values:

Grain size (millimeter)	*Percent larger than*
2.38	1.01
1.168	6.68
0.589	27.08
0.297	72.93
0.149	95.66
0.074	99.30

The defining parameters of the experimental sand in Krumbein's notation are, $d_{GM}=0.42$ millimeter and $\sigma_{\varphi}=0.96$. (See fig. 3.)

The quantities observed during a test are shown in figure 4, which is representative of the basic data. The envelopes of the wave crest and trough, the undisturbed water surface, and the initial beach profile were marked on the glass tank wall, then transferred to a graph. The point of impending wave break, point S_1 in figure 4, was believed to be significant and was noted. At the point of impending wave break the wave front in the immediate vicinity of the crest is almost vertical and the water particles on the crest are moving with a velocity slightly below the velocity of wave propagation. As motion continues the crests deform rapidly, then break. It will be shown later that the transport of sand at the point of impending wave break is a maximum.

In the tests made with the small tank, the gradual formation and stabilizing of the bar was observed through the glass wall. Roughly speaking, stability was reached in one hour with a slope of 1 on 15, in two hours with a slope of 1 on 30, and in 4 hours with a slope 1 on 70, the time intervals being the duration of the respective tests made in the small tank. It was not possible to observe the formation of the bars during the tests made in the larger tank; therefore, the time intervals for those tests were determined from the values obtained for tests in the smaller tank by comparing wave lengths and using a transference equation based on the Froude number. The minimum

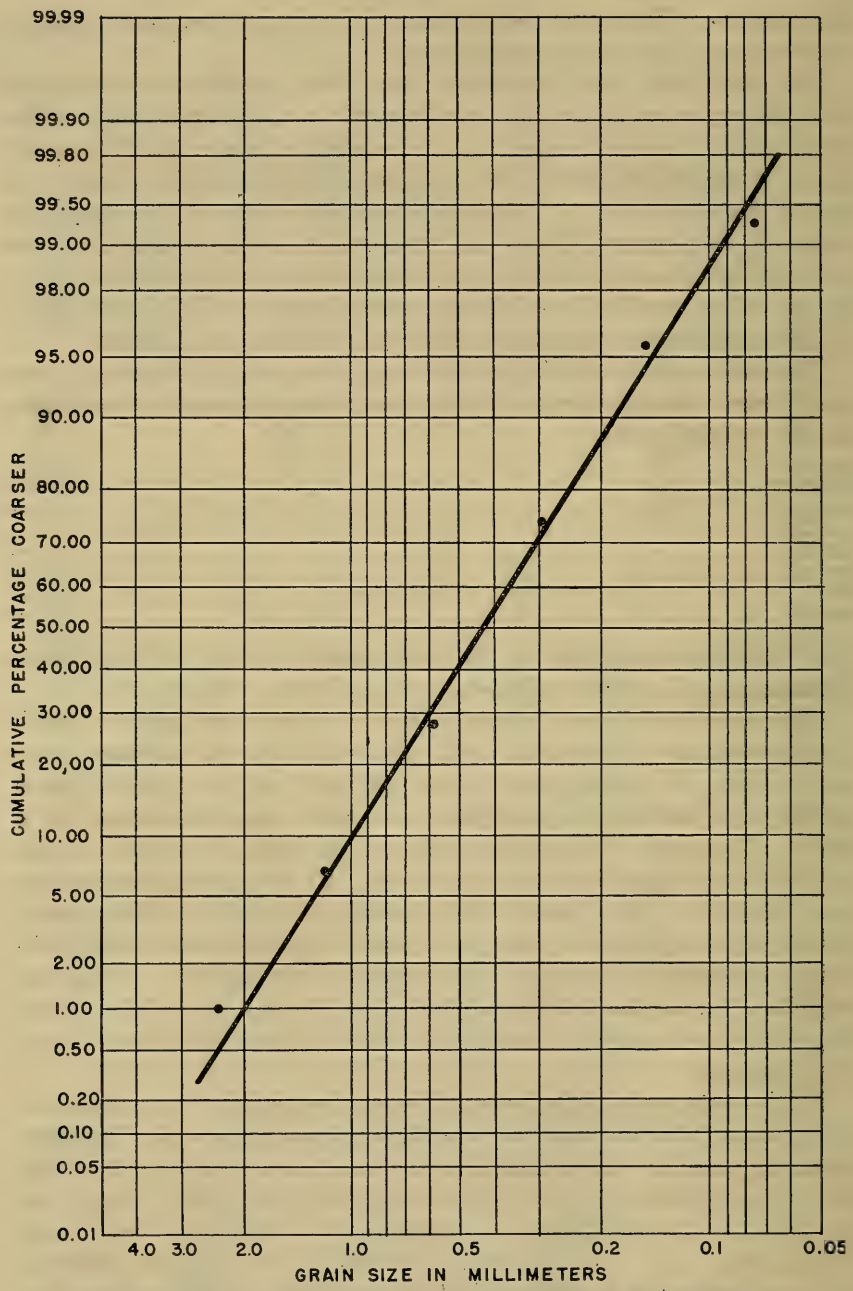

ANALYSIS OF SAND USED IN EXPERIMENTS

FIGURE 3.

test durations adopted for the larger tank on this basis were 4 hours for the slope 1 on 30, 8 hours for the slope 1 on 50, and 12 hours for the slope 1 on 70.

The configuration of the bar shown in figure 4 is indicated by a smooth curve. This is an idealization in that the bar surface and the adjacent bottom actually were covered with ripple-marks. The curve shown was derived from master traces of the actual surface; it and similar data are the average of two or more runs.

It is desirable to define the waves reaching the experimental beach in terms of their deep-water characteristics but the waves generated in both the small and large tanks were shallow water waves. Since the period is constant, the wave length, λ, and the wave height, a, may be related to the corresponding deep water characteristics λ_o and a_o by the following approximate expressions: $\frac{\lambda}{\lambda_0}=tanh\,\frac{2\pi H}{\lambda}$

$$\frac{a_o}{a}=\left(\frac{2\pi H}{\lambda}+sinh\,\frac{2\pi H}{\lambda}\,cosh\,\frac{2\pi H}{\lambda}\right)\Big/cosh\,\frac{2\pi H}{\lambda} \qquad (10)$$

where λ and a are measured at a point having the undisturbed water depth H (reference 7). The elimination of H between equations 1 and 2 gives an expression for the dependence of a_o/a upon λ/λ_o. This expression is shown graphically in figure 5 and is the basis of the desired reductions. Taking the observed value of the wave period, T, the deep water wave length λ_o may be computed from

$$\lambda_0=gT^2/2\pi \qquad (11)$$

The value a_o/a corresponding to the ratio λ/λ_o where λ is the measured wave length in front of the wave generator, may be read from the curve in figure 5. Knowing the value of the ratio a_o/a, the deep water wave height a_o, is readily obtained since the wave height a measured in front of the wave generator is known. These computations were made for all the tests.

Section IV. RESULTS OF LABORATORY EXPERIMENTS

The initial changes in the form and movement of the bar are illustrated in figure 6 which shows a typical bar development. The form and movement changes do not progress uniformly with time, but oscillate about mean values. The inset on figure 6 is a smooth curve representing the average position of the bar with time. The initial assumption as set forth in section II*a*, to the effect that the motion of the bar is decreased to an imperceptible value is thereby shown to be substantiated by the laboratory observations.

806229—48——3

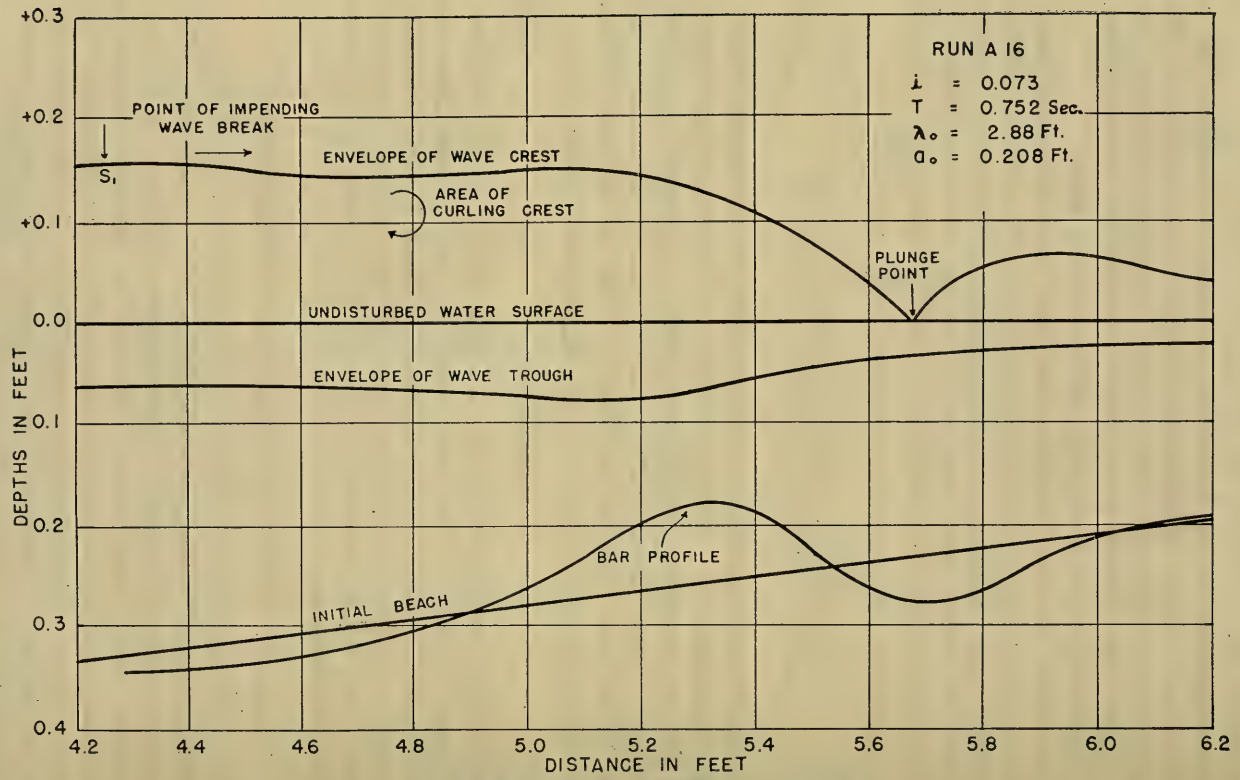

EXAMPLE OF GRAPHIC DATA

FIGURE 4.

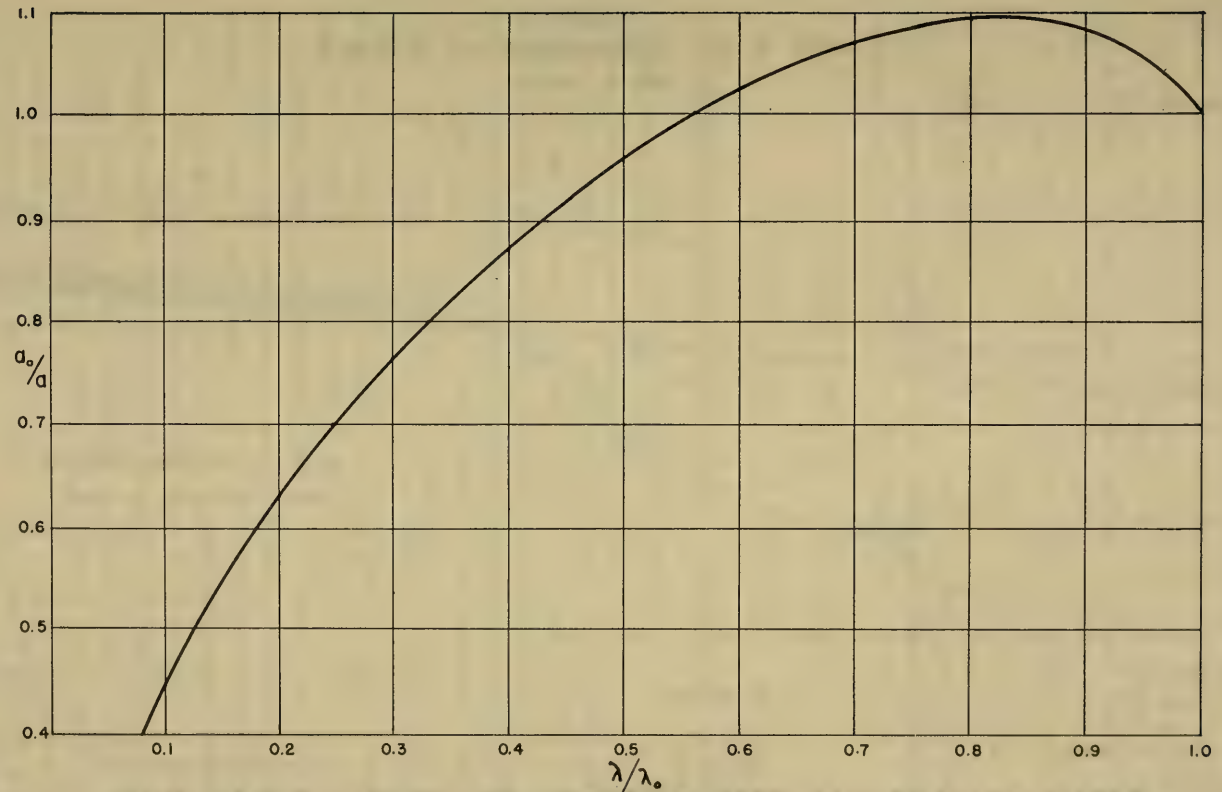

WAVE HEIGHT – LENGTH RELATIONS IN DEEP AND SHALLOW WATER

FIGURE 5.

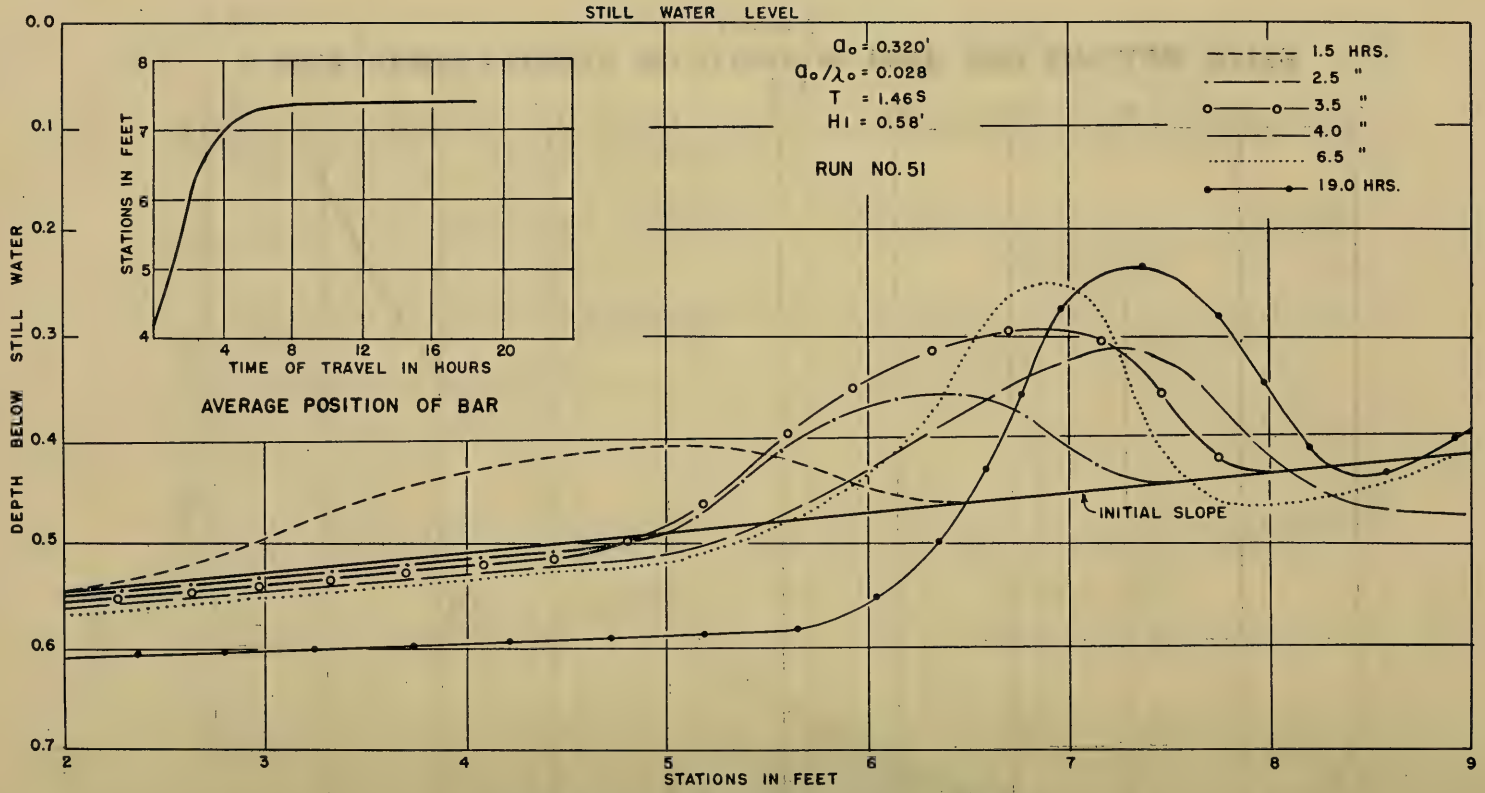

STAGES IN FORMATION OF A BAR

FIGURE 6.

The factors controlling the position of the bar at the time it becomes relatively stable are stated in equation 4. The results of the tests to evaluate the terms in equation 4 are plotted on figure 7. Figure 7A shows the relation between a_o/H_B i. e., the ratio of wave height to the depth of bar base; and the wave steepness, $a_o\lambda_0$.

It appears that for the same value of wave steepness, a_o/λ_0, the initial slope i, of the beaches did not affect the ratio a_o/H_B. If an effect is present, it is of the order of the error of observation.

Since the points are plotted without differentiating between the values of the ratio $\frac{\lambda_0}{d_{GM}}$ and do not scatter to any great extent, it may be concluded that the effect of this ratio, if present, also cannot be larger than the observation error. For example, considering the following pair of data taken from the records:

$$\lambda_0=48 \text{ ft.}, \; a_o/\lambda_0=0.06, \; a_o/H_B=0.50$$

$$\lambda_0=18 \text{ ft.}, \; a_o/\lambda_0=0.06, \; a_o/H_B=0.45$$

a 300 percent variation is indicated in the $\frac{\lambda_0}{d_{GM}}$ values, yet the variation in the values of the ratio a_o/H_B is only 10 percent.

Interpretation of the curve in figure 7A leads to the conclusion that if the water depth remains constant, the depth of bar base and consequently, the position of the bar, formed by a single system of waves is a function of the wave height, a_o, and wave steepness a_o/λ_o. If the water depth and wave steepness are held constant, an increase in the wave height will move the bar seaward. Furthermore, if the water depth and wave height are held constant, an increase in the wave steepness will move the bar shoreward. Further, if the wave height and wave length are held constant, H_B, will likewise remain constant, and any increase in the depth of water moves the bar shoreward.

In figure 7B the data from the beaches of different slopes are plotted individually. No distinction is made, however, between the tests made in the large and small tank. Similarly, no differentiation is made between points associated with the variable sand parameter, λ_0/d_{GM}. It should be noted that the ratio of the depth of bar crest to the depth of bar base H_c/H_B, is practically independent of the wave steepness ratio a_o/λ_0, and of the slope i. Since the data covers a wide variation in the values of the ratio λ_0/d_{GM}, it may also be inferred that the ratio H_c/H_B is likewise independent of the ratio λ_0/d_{GM} within the order of the error of the observations. The data as plotted in figure 7B give a constant value

$$H_c/H_B=0.58 \tag{12}$$

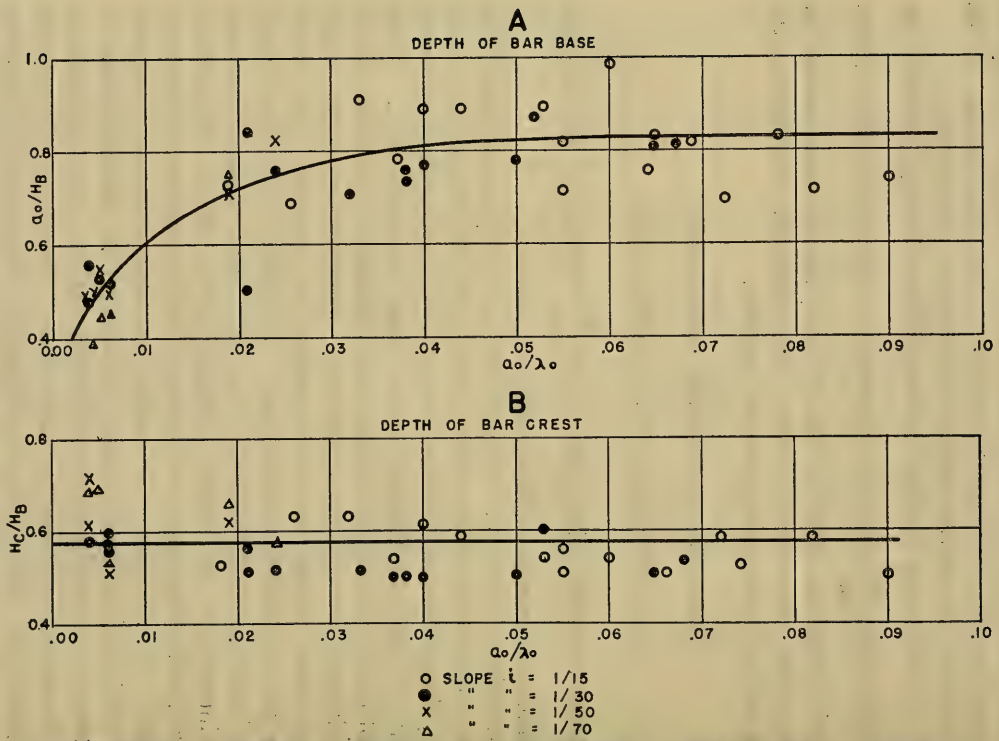

RELATION BETWEEN BEACH SLOPE, WAVE HEIGHT AND LENGTH, DEPTHS OF BAR CREST AND BASE

FIGURE 7.

In examining the forms of the bars obtained in the laboratory on the basis of equation 9 to determine the importance of a_o/λ_0, it is desirable to replace the bar base depth H_B with the depth of the initial beach surface H'_B measured at the point just below the crest. See figure 1. This substitution is useful because H'_B is more accurately determined than H_B and is permissible because the ratio H_B/H'_B approximates a constant quantity, which is a function of the slope i.

Figure 8 gives the results of data obtained in the small tank for a slope of 1/15. The values of λ/H'_B as plotted in figure 8 were grouped and averaged for certain intervals of the wave steepness ratio. No systematic variation in the configuration of the bars with wave steepness is discernible. Therefore a single curve passing through the points may be considered as defining the form of the bar for this slope ($i=1/15$). The results indicate that the form of the bar is apparently independent of the size of the generating waves. The bar base and the initial beach surface also are shown in the same figure. It is seen that here $H_B/H'_B=1.2$. This ratio differs from unity due to the fact that the slope of the initial beach surface is steep and the bar troughs have descended relatively far below the initial surface. A similar analysis of the bar form developed in tests made on beaches with a 1/30 slope leads to the same conclusion; i. e., the form of the bar is independent of the wave steepness ratio. The ratio H_B/H'_B in this case has the value of 1.09, indicating that although the troughs of the bar descend below the initial surface, the effect is not so pronounced as that obtained with the steeper slope, $i=1/15$.

The results of the test with 1/70 beach slopes are shown in figure 10. In this case the effect of wave steepness is noticeable. Bars formed by waves of small steepness ratio have wider crests and longer bar bases. With an increasing steepness ratio the bars become slender and pointed.

An examination of figures 8 and 9 shows that in the bar environment of beaches having steep slopes the troughs descend markedly below the level of the initial undisturbed beach. In the bar environment of beaches having flat slopes the troughs hardly descend below the level of the undisturbed beaches. As a result of this behavior, the trough depth below the undisturbed water surface manifests a remarkably uniform relationship with the depth of water over the bar crest.

Let H_t denote the depth of the trough below still water level. The dependence of H_t/H_c on a_o/λ_o is indicated in figure 10. To facilitate the comparison the data for the different slopes are shown separately. It is seen, making due allowance for errors of observation, that H_t/H_c is practically independent of wave steepness and of beach slope. The ratio is found to have an average value of 1.69.

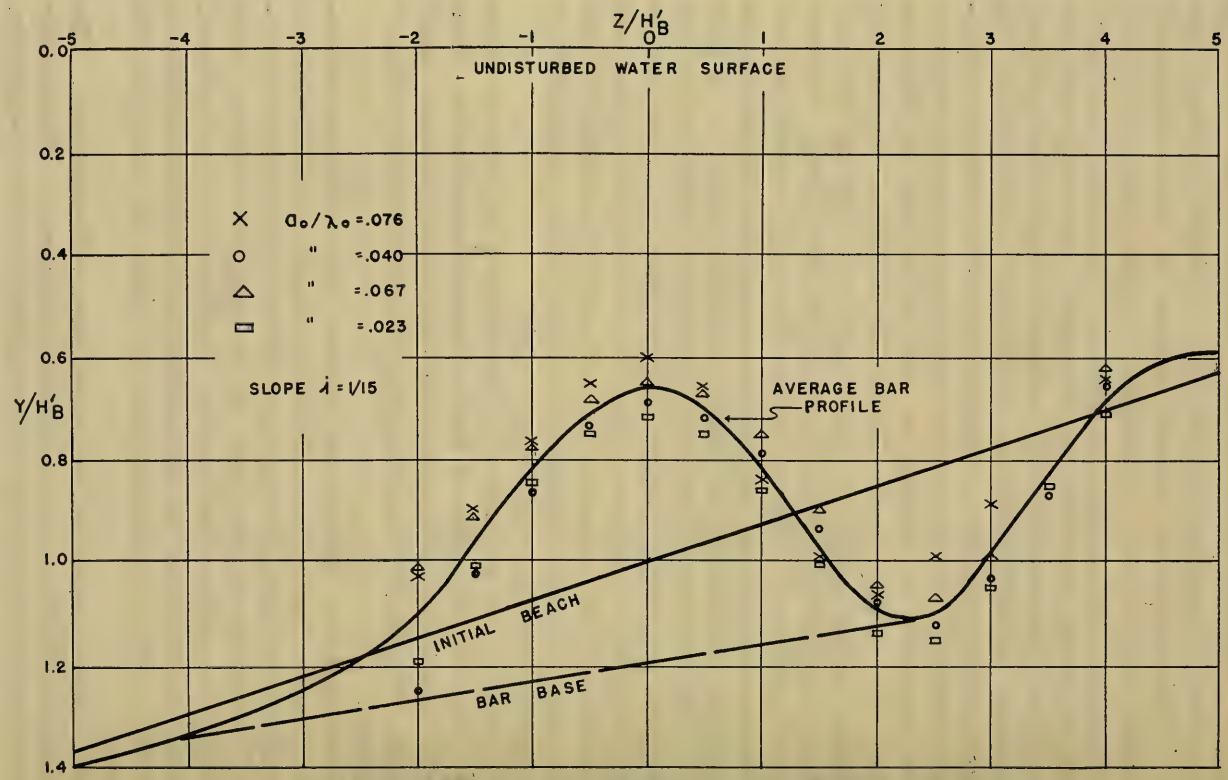

CONFIGURATION OF BAR ON A STEEP BEACH

FIGURE 8.

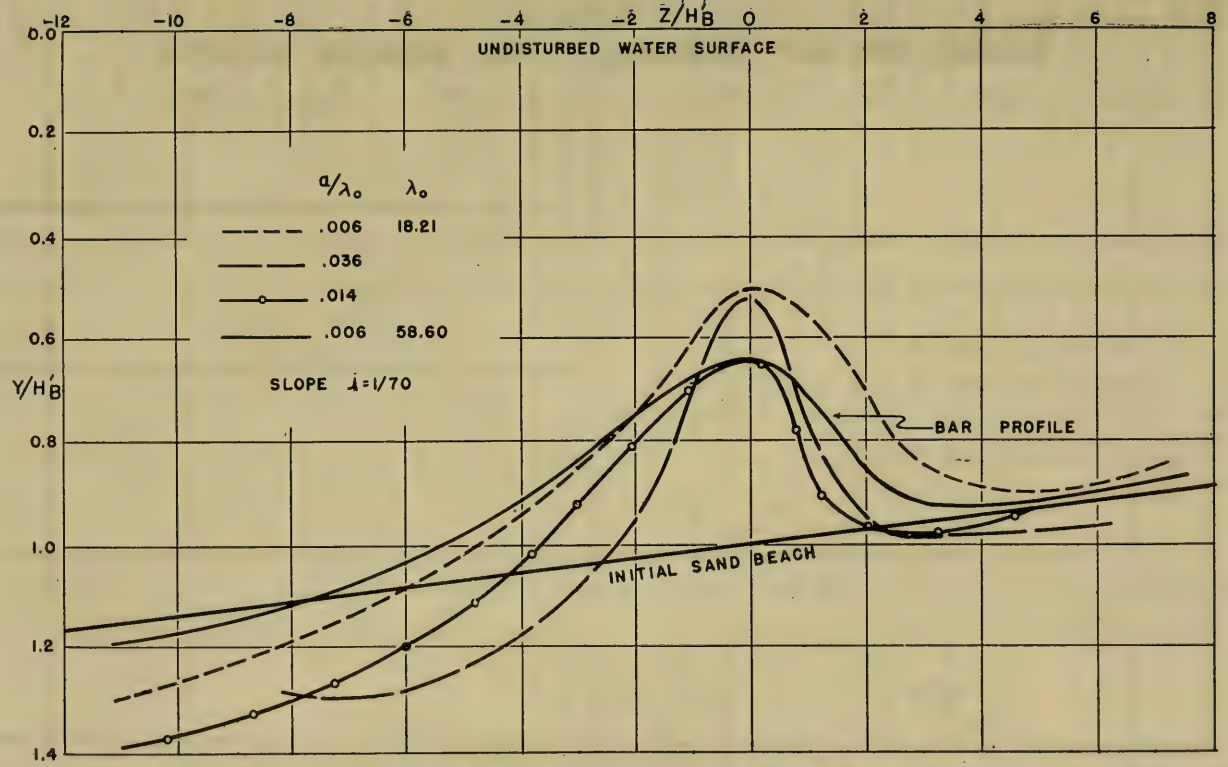

CONFIGURATION OF BAR ON A FLAT BEACH

FIGURE 9.

80023—45——4

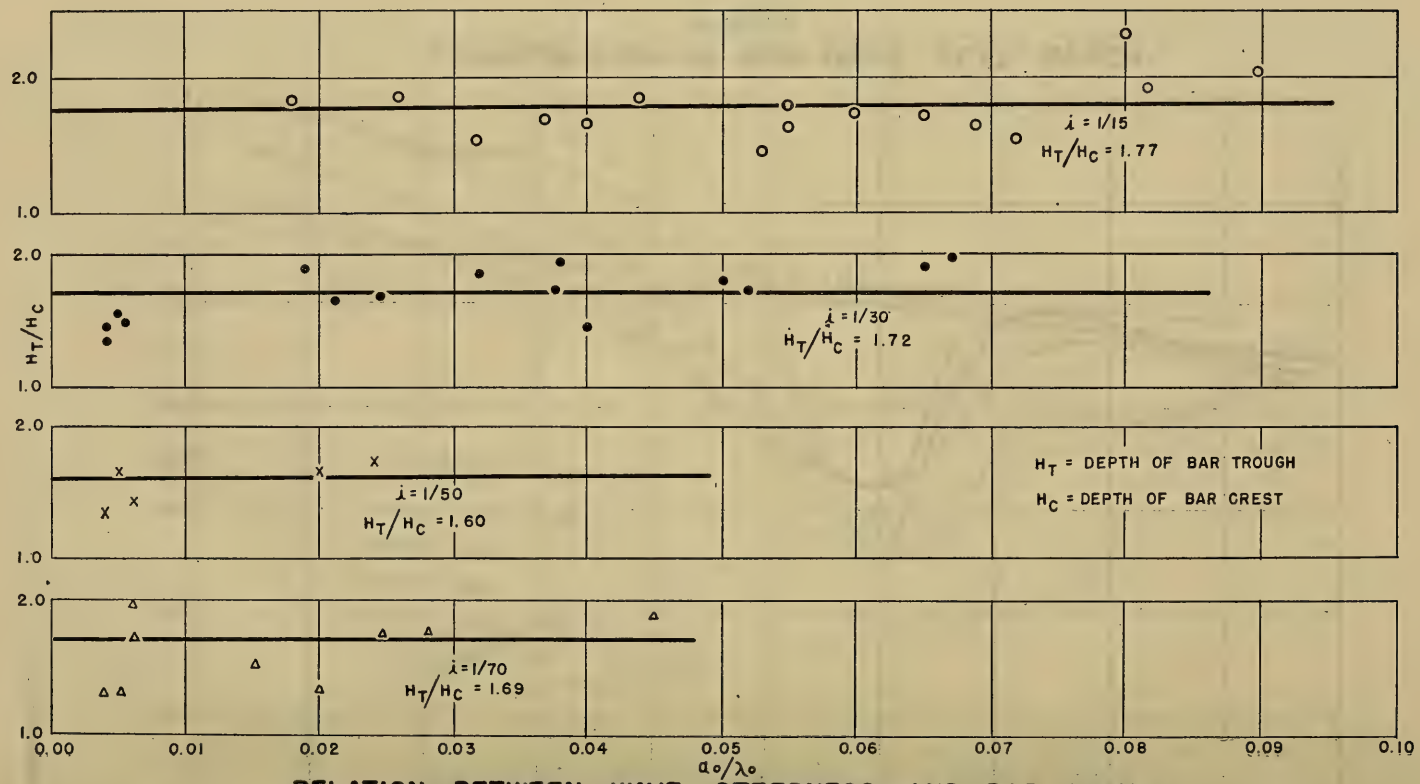

RELATION BETWEEN WAVE STEEPNESS AND BAR DEPTHS

FIGURE 10.

Section V. FIELD OBSERVATIONS

A. *Form and dimensions of natural bars.*—The bars of the Pomeranian coast have been sounded by Otto and Hartnack (references 2 and 4), and the latter's paper includes records of soundings by Lehmann and others. Evans (reference 5) measured the bars of Lake Michigan. The data from these investigations will be examined here to ascertain whether any similarity exists between the form of natural bars and those developed in laboratory tests.

Consider the profiles of Lake Michigan bars shown in figure 11, from which two groups of bars are selected; one consists of the bars in a first zone of the four profiles, i. e., the bars closest to the shore and the other, those in a second zone the next seaward. The bar base depth H_B of each bar was determined, and the distance y and z of profile points of a given bar obtained, from which the space parameters y/H_B and z/H_B are formed. The averaged and smoothed values of these parameters for the bars of the two groups are shown in figure 12. The values are plotted as rectangles for the first zone and circles for the second zone. Since the distribution of points for the two zones is approximately the same, a mean curve can be drawn as shown in the figure. The curve may be representative of the bars of Lake Michigan. In preparing the Pomeranian coast data, the average for the given locality was taken irrespective of the zones of bars. These data are represented by dots, triangles and crosses and the mean curve through the points is representative of the bars of the Pomeranian coast. The lowest curve represents the average value for the bar determined by the experiments based on the data shown in figure 9.

The form of the experimental bars varies considerably from that of the natural bars. The natural bars are flatter and longer than the experimental bars; significantly, however, the depth of the crests expressed as a fraction of the depths of bar base have practically the same value for the natural and the experimental bars.

No adequate explanation can be offered now as to the cause of the difference in the forms of the natural and experimental bars, except to suggest that the waves producing the natural bars are of a mixed type, and the order and extent of turbulence is of a different scale resulting in a difference in the suspension and motion of particles. It is believed that such factors would tend to produce flatter bars.

A more detailed comparison of the crest and trough depths of the natural bars is given in table 1. The sequence of bars defines the zones in which the bars occur, the bar nearest shore lying in the first zone.

TABLE I.—*Crest and trough depths of natural bars*

Locality and investigator	Average slope	Factor	Zone			
			I	II	III	IV
Pomeranian Coast (Otto)	0.013	H_B/(ft.)		3.8	6.5	
	.013	H_C/H_B		.46	.57	
	.013	H_t/H_C		1.79	1.56	
Pomeranian Coast (Lehmann)	.017	H_B/(ft.)	3.12	5.74	10.40	14.8
	.017	$H/_CH_B$	.54	.55	.57	.58
	.017	H_t/H_C	1.71	1.50	1.66	1.56
Pomeranian Coast (Otto)	.014	H_B (ft.)		7.02	12.20	20.8
	.014	H_C/H_B		.46	.52	.52
	.014	H_t/H_C		1.87	1.77	1.81
Pomeranian Coast (Hartnack)	.017	H_B (ft.)	2.22	6.56	9.88	13.1
	.017	H_C/H_B	.42	.49	.55	.62
	.017	H_t/H_C	1.86	1.77		
Lake Michigan (Evans)	.017	H_B (ft.)		7.12	13.37	20.6
	.017	H_C/H_B		.55	.62	.62
	.017	H_t/H_C		1.45	1.42	1.55

The dimensions shown are average values derived from different profiles for natural bars found in similar zones. The bar nearest the shore is designated as being in the first zone, but at times it was difficult to recognize that zone. Therefore, in some cases the zone designation may not be correct. The data in table I, as would be expected, indicate that the depth of the bar base increases with the order of zones. The ratio of the crest depth to the bar base depth tends to increase as the distance the bars lie from the shore increases. This may indicate that the bars that are farther away from the shore have lost material from their surface. It is possible, also, that the larger waves do not operate long enough in this area for the complete formation of bars. The mean value of H_C/H_B when computed from the table is 0.54 which compares favorably with the corresponding ratio, H_C/H_B of 0.58, obtained from the laboratory tests. For the different determinations the ratio of trough depth to the bar crest depth varies between 1.42 and 1.86. The average value H_tH_C of 1.66 compares well with the average of the laboratory determination; H_t/H_C of 1.69.

B. *Lake Michigan bars and observed waves.*—The profiles of the bars of Sylvan Beach, near the White Lake piers on the eastern shore of Lake Michigan, were measured by Evans in 1939 (reference 5). Some of these measurements are reproduced in figure 11. The essential bars in a given profile are three in number, ignoring the indefinite forms near the shore. An application of the results shown in figure 7A might be to determine the magnitude of the waves necessary to produce those bars. The underlying supposition is, of course, that each bar in a given profile is created under the action of a singular system

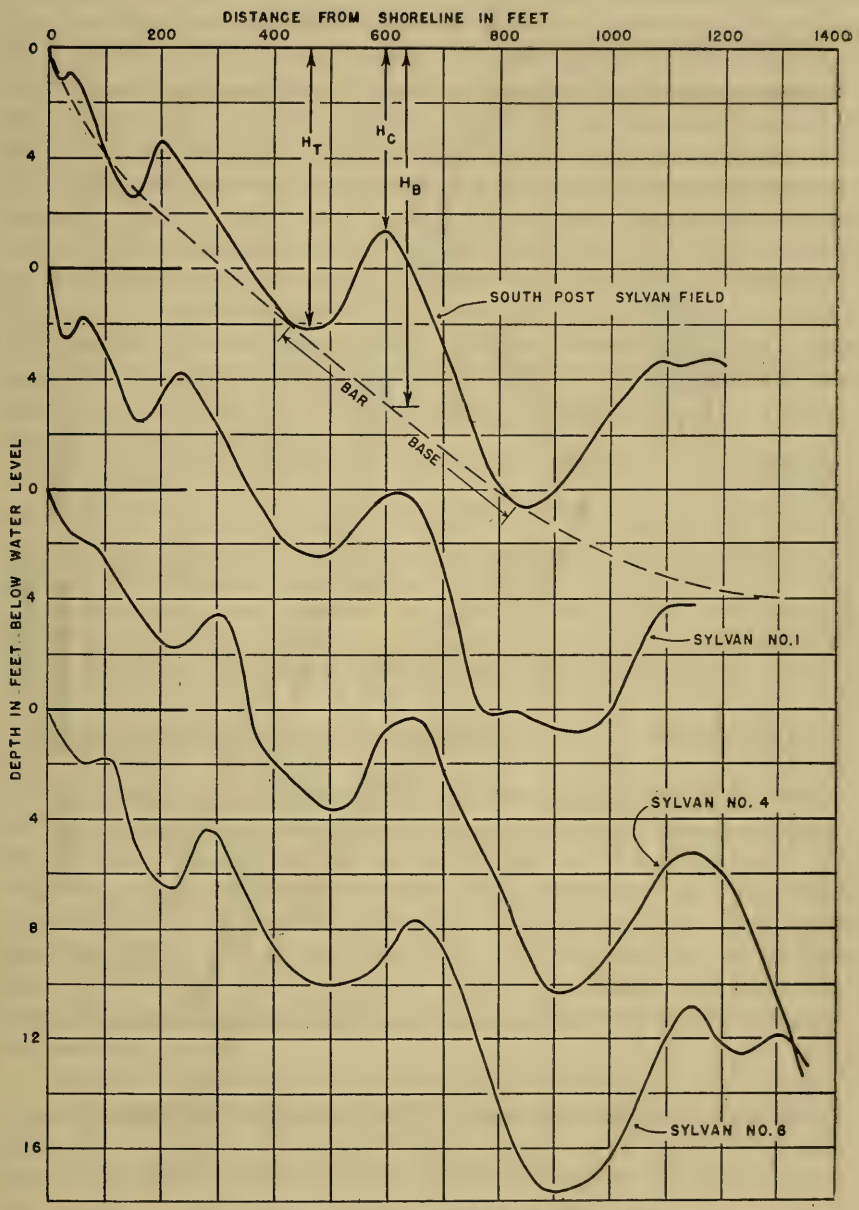

BAR PROFILES, LAKE MICHIGAN

FIGURE 11.

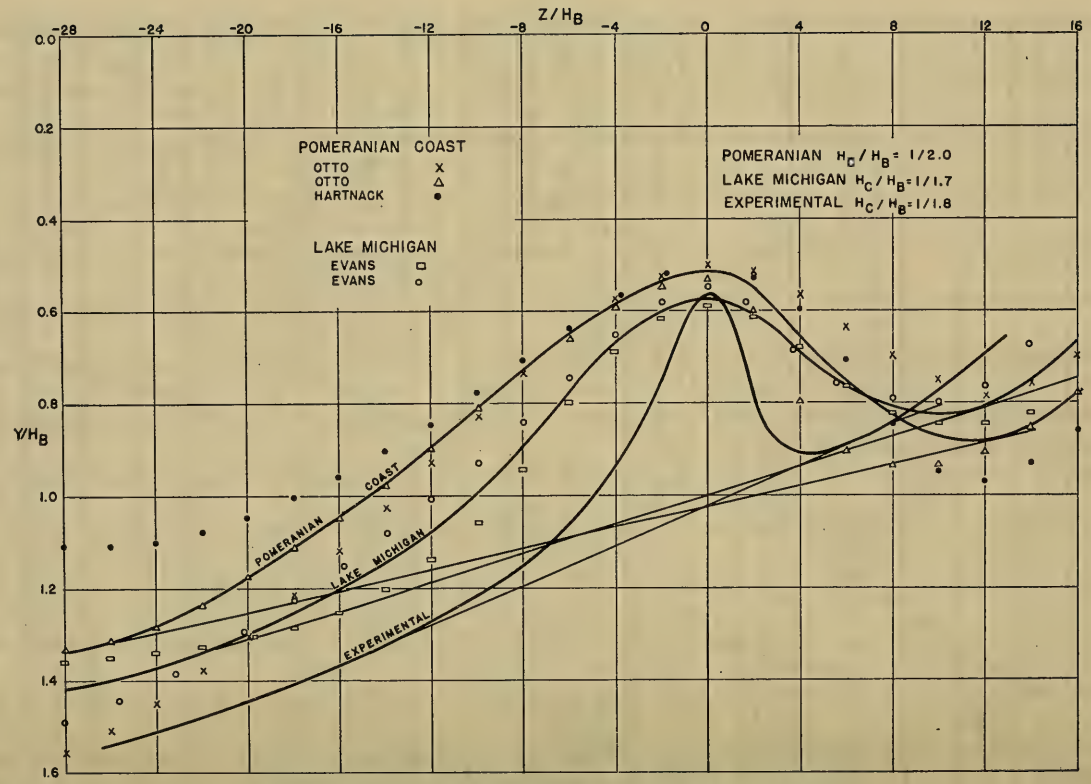

AVERAGE CONFIGURATION OF NATURAL BARS

FIGURE 12.

of waves, and the respective wave systems are different. It is recognized that natural conditions may not approximate this supposition. The bar base depths of the bars in the different zones are defined by lines joining the troughs of the bars. According to the definition, the segment of the line under the body of a given bar becomes the bar base. From figure 11 the average value of the bar base depth, H_B for the bars in the first zone of the profiles is 7.2 feet; in the second zone, 13.2 feet; and in the third zone, 19.5 feet. If it be assumed, for example, that the bars are formed under waves of steepness ratio $a_o/\lambda_0=0.03$, the required value a_o/H_B from figure 7A is 0.75. Accordingly, the bar of the first zone required 5.4-foot waves for its formation, that of the second zone required 10.5-foot waves, and the third zone 14.5-foot waves. H. A. Montgomery observed wave heights in Lake Michigan, near Milwaukee, from 10 April 1931 to 28 September 1932 (reference 7). The maximum wave heights recorded over the first 12 months of the investigation were:

Maximum wave height (in feet)	*Number of days on which recorded*
14	1
13–14	0
12–13	0
11–12	1
10–11	2
9–10	7
8–9	6
7–8	5
6–7	22
5–6	32
4–5	48
3–4	71

The average period of the waves of lowest height was 4.3 seconds, with a minimum period of 3.5 and a maximum of 5.0 seconds. Since the water at the location of the measurements was quite deep, the inference is that the low waves were about 95 feet long. The wave steepness ratio was about 0.03. The above measurements were made on the western shore of the Lake. If they apply to the eastern shore near White Lake, the waves are of the order of magnitude expected to create bars of the dimensions observed in the first and second zones.

The above comparison of laboratory experiments and natural processes would be of greater value were it possible to discuss simultaneously the effect of a spectrum of waves operating over a beach. Actually it may be surmised that waves in nature are far from a singular system.

Section VI. FACTORS AFFECTING MECHANISM OF BAR FORMATION AND MOVEMENT

As stated in the introduction, certain observations of the mechanism of bar formation and movement were made during the course of the experiments. While these observations are somewhat limited it is believed that they are of sufficient value to justify some discussion.

A. *Sand transportation on smooth beaches.*—A qualitative measure of the bed motion of sand in the initial and the final stages of bar formation was obtained from an experiment in the small tank with a 1 on 70 slope, wave height of 0.32 foot, and wave period of 1.4 seconds. The undisturbed water depth H_1, at the point where waves began to deform was 0.58 feet. In figure 13 are shown the initial condition of the beach, and the envelopes of the wave crests and troughs. The breaker was of the spilling type and was completed at station 4. In figure 14 are shown the last stages of the bar formation and the corresponding envelopes of crests and troughs. Very marked changes are noticeable both in the beach surface and the water surface. Ripple marks in the area in front of the bar are in evidence. The general slope of this area is almost horizontal. The breaker, now of the plunging types, has moved toward the shore. It is important to note that the bar was formed, not where the breaker was initially present, but appreciably nearer the shore.

Determinations of the rate of transportation of sand were made for the initial and the final conditions of the beach. Initially measurements were made with galvanized rectangular traps, one-half inch wide, one inch deep, and extending across the tank. Four of these traps were set level with the sand surface at one-foot intervals to collect the sand in motion along the beach. Samples were collected for selected intervals and the locations of the traps were changed periodically so as to obtain the rate of sand transportation over a stretch of 13 feet between the stations *0* and 13. The data thus obtained are shown graphically in figure 15 on which the rate of sand transportation, Q, is plotted against the station distances. The rate is expressed as pounds per hour per foot of width. On the graph are shown the location of the breaker as it initially occurred and the final position of the bar.

The maximum rate of transportation of sand on the initial smooth beach in the area investigated occurred at the point of impending wave break. Considerable movement of sand was observed along the beach surface where the waves were breaking. The breaker was of the spilling type, and the distinctive discontinuity of the plunging type of breaker was lacking. The bar is eventually formed at a point where the rate of sand transportation is nearly a minimum. Movement of sand occurs on the beach up to the limit of wave action.

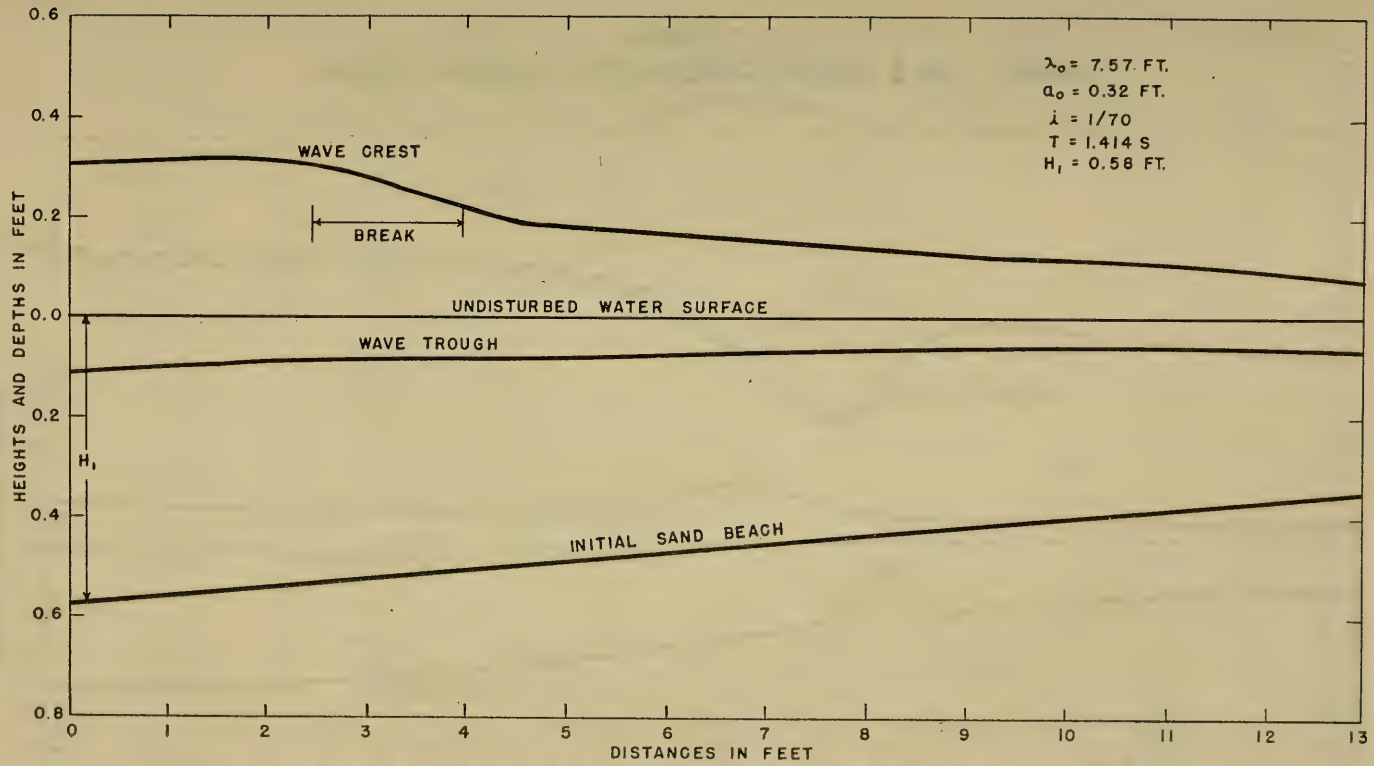

WATER SURFACE ELEVATIONS FOR INITIAL CONDITIONS

FIGURE 13.

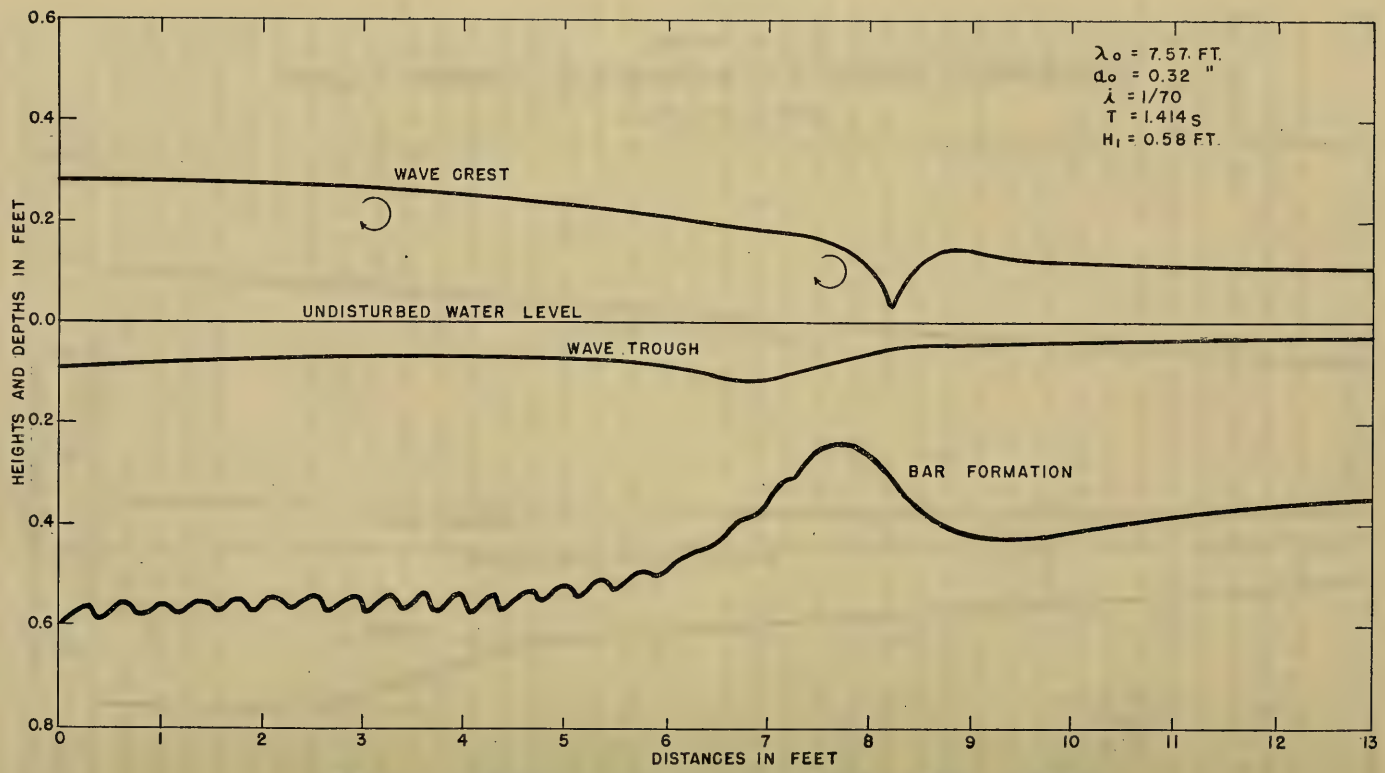

WATER SURFACE ELEVATIONS WITH BAR FORMED

FIGURE 14.

Obviously, the non-uniform transportation of sand is effected by the total displacement of the water surface at a given point during the passage of waves. If ΔH_1 is the maximum elevation of the surface above the undisturbed water level during the passage of the waves and ΔH_2 the maximum depression, the total displacement is given by $\Delta H = \Delta H_1 + \Delta H_2$. The relation between the rate of initial sand transportation and the fall of the water surface is shown in figure 15. It is apparent that correlation exists between the rate of sand transportation and the total displacement of the water surface during the wave passage. A clear picture of the correlation of surface displacement with the rate of sand transport is obtained by considering the dependence of the rate of sand transportation Q, upon ΔH expressed in terms of dimensionless quantities. Three distinct regions must be kept in mind in dealing with the problem of sand transportation under wave action. The most important region has been referred to previously as the bar environment, which is bounded seaward by the point of impending wave break and shoreward by the point of reformation of waves beyond the breaker; the limits of this region are readily obtained in laboratory experiments. The remaining two regions are: the one extending indefinitely seaward from the point of impending wave break; the other extending to the shore line from the point of reformation of waves. The laws of transportation of sand in these regions are expected to be different.

In this investigation only the movement of material in the region of bar environment under initial conditions will be considered. The assumption is made that the rate of sand transportation Q depends on the total surface displacement ΔH, the depth of water H_1 at the point of impending wave break; the period of the wave T; the characteristic sand grain size d_{GM}, the kinematic viscosity ν; the densities of water and sand ρ_w and ρ_s, respectively; the gravity constant g; the slope i; and the sand dispersion coefficient σ_φ. The ordinary arguments of dimensional analysis result in the general relationship

$$\frac{QT}{\rho_s g H_1^2} = f\left(\Delta H/H_1,\ \rho_w/\rho_s,\ \frac{\sqrt{gH_1}\,d_{GM}}{\nu},\ H_1/gT^2,\ d_{GM}/H_1,\ i,\ \sigma_\varphi\right) \quad (13)$$

defining the law of sand transportation. In the equation the dimensions of the initial deep water waves are missing, since the wave characteristics are determined by T and ΔH. The last six quantities may be considered constants for a given test hence it suffices to write

$$\frac{QT}{\rho_s g H_1^2} = f(\Delta H/H_1) \quad (14)$$

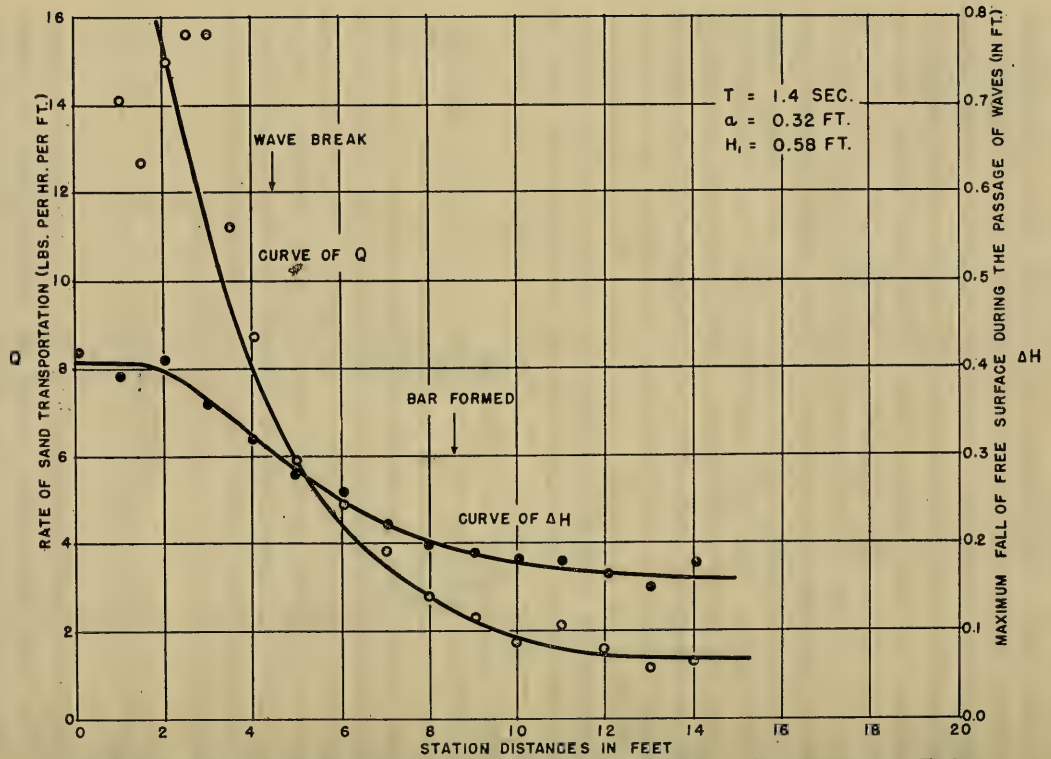

RELATION BETWEEN RATE OF INITIAL SAND TRANSPORTATION AND FALL OF WATER SURFACE

FIGURE 15

Figure 16 is plotted in accordance with the latter equation from figure 15. The product $\rho_s g$, being the specific weight of sand, is taken to equal 137 pounds (weight) per cubic foot. The quantities Q and ΔH are read from the curves in figure 15. Since Q was expressed as pounds (weight) per foot width per hour and T is given in seconds, the numerical value of QT involves the ratios of two different units of time. Interpretation of the curve reveals that the rate of sand transportation in the bar environment is controlled, among other things, by the total displacement of the water surface, ΔH and that there is a critical displacement value below which no appreciable transportation of sand is possible.

Further conclusions cannot be drawn on the basis of the meager data available, but the problem is important enough to warrant a separate and a more complete study. In an extended study the effects of all the parameters entering into the right hand side of equation 14, should be examined.

B. *Sand transportation and sand ripples.*—The discussion of sand transportation given above refers to the initial conditions when the beach is smooth and the slope of the surface is constant. Certain changes in the beach surface occur as transportation continues. See figure 14. Sand accumulates in the process of bar development and sand ripples appear seaward of the bar. The effects of these two changes are quite significant. With the formation of the bar the breaker characteristics are changed, the total displacement of water surface in the area between the breaker and the point of impending break of the waves becoming nearly constant everywhere in this area. The sand ripples signify a new mode of sand movement and a very considerable reduction in the rate of sand transport, as will be shown.

Sand ripples begin to form in the area just under the breaking wave, apparently from two causes. One is the secondary undulations, which manifest themselves at the surface of the breaker and are transmitted to the bottom to form corrugations. The other is an accidental unevenness of the bottom surface due to nonuniformity of resistance of the sand or some other discontinuity of the bottom geometry. Once the sand ripples have been started, in one way or another, a continuous series of them results under favorable conditions. Their final dimensions are controlled by the depth of water, the period of the waves, the total displacement of the water surface during the passage of waves, and the size and dispersion coefficient of the sand.

Movement of sand in the bar environment after sand ripples have covered the entire beach surface appears to take place in the following manner. At the instant that a crest is moving over a sand ripple, the motion of water particles just above the ripple is toward the shore. At this moment the sand of the ripple surface is moved toward the

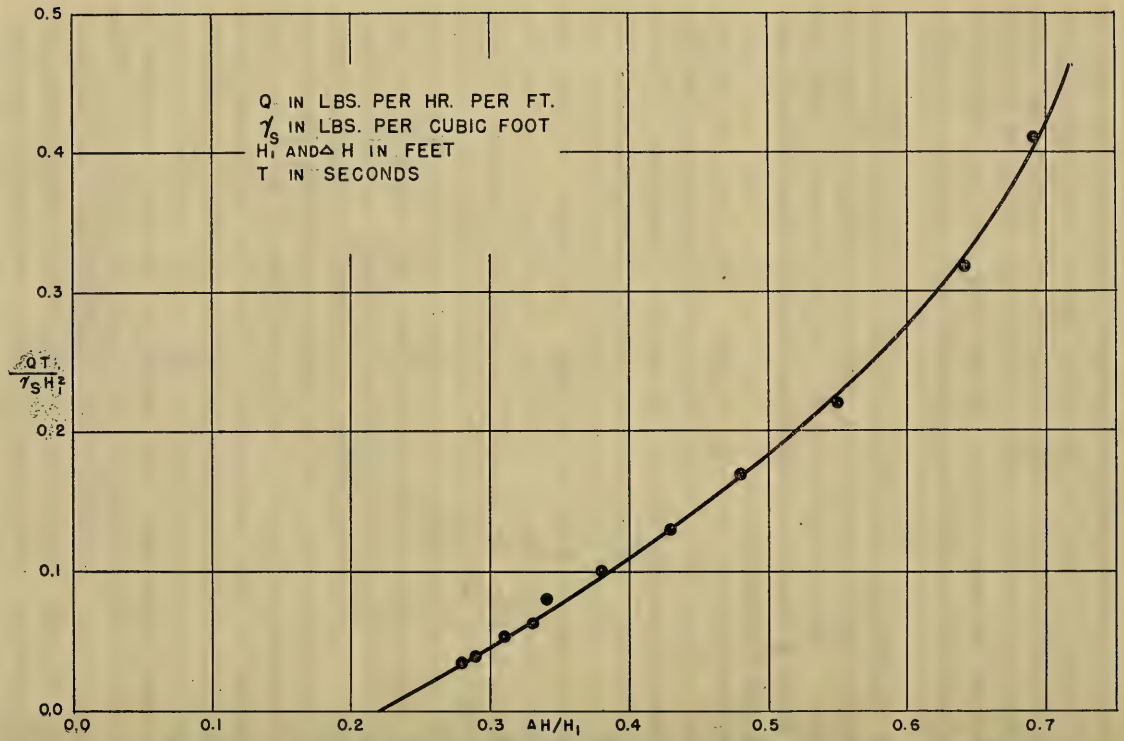

QUANTITY OF SAND TRANSPORTED IN BAR ENVIRONMENT FOR INITIAL CONDITIONS

FIGURE 16.

crest of the ripple and then downward into the depression of the next ripple. See figure 17. Simultaneously an eddy is formed in the depression and is loaded with small sand particles picked up from the depression. The hydrodynamic reaction between the rotating eddy and the sand surface ejects the eddy together with its sand particles upward some distance. With the trough of the wave following, the movement of water particles near the sand ripple surface is reversed. This moving mass of water carries with it toward the sea the suspended sand particles of the previous eddy. In this reversed motion the major portion of the suspended particles is deposited on the surface of the sand ripple from which it initially derived and a minor amount is taken over the next ripple on the seaward side. The cumulative effect of this cyclic process is that a ripple moves gradually by small steps toward the shore. In the process the larger particles of sand of the environment are taken to the shore and the lighter particles, through suspension, are taken to sea. Thus the sand ripple, rather than its motion, becomes the sorting agent.

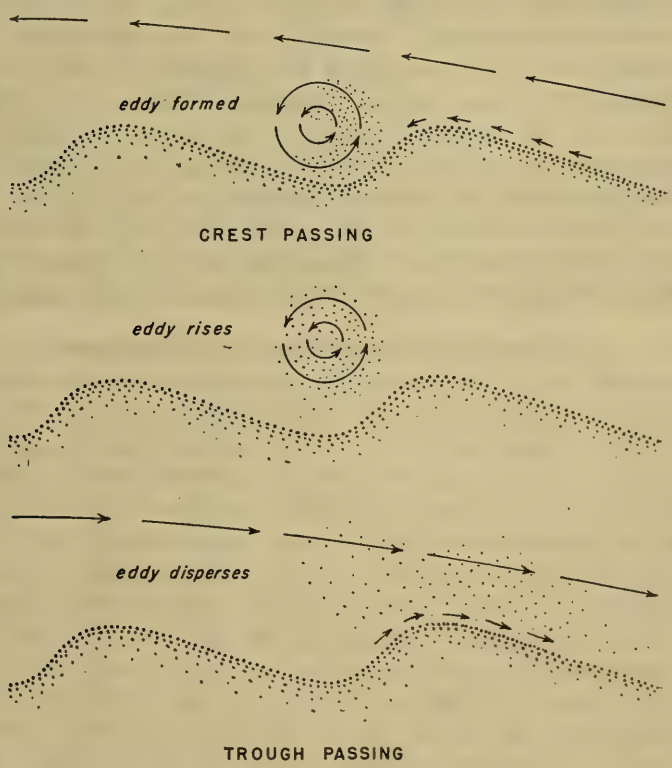

MECHANISM OF MOVEMENT OF SAND OVER SAND RIPPLES

FIGURE 17.

The net rate of sand transportation in the form of ripples can be ascertained once the distance traveled by the ripple and the area of the vertical section of the ripple is known. Let Q_r denote the weight of sand transported per hour per foot of width. Denoting the distance traveled by a sand ripple per hour by D and the sectional area by A,

$$Q_r = \gamma_s DA \tag{15}$$

where γ_s is the specific weight of sand. For the sand ripples in test 51

$$A = 0.54hl \tag{16}$$

where h is the height of the ripple mark and l the length of the base, both quantities being expressed in feet. Accordingly,

$$Q_r = 0.54hlD\gamma_s \tag{17}$$

Table 2 lists the dimensions of some thirteen sand ripples of test 51 together with their rate of travel. The first ripple mark was located at station 2, and the remainder covered the distance between the bar and that station. See figure 14. It can be seen from the table that with a few exceptions the ripples have nearly equal sizes and travel with nearly equal velocities. This can be explained on the basis that the depth of water over the ripples is constant and the displacement of the surface uniform during the passage of waves. On the average the rate of transportation of each is $Q_r = 1.21$ pounds per hour per foot of width. Comparing this with the data of figure 15 it is obvious that sand transportation in the form of ripples is much smaller than the sand movement under initial conditions.

TABLE II.—*Transportation of Sand by Ripples*

No.	l	h	D	Q
	Ft.	*Ft.*	*Ft./hr.*	*Lbs./hr./ft.*
1	0.31	0.06	0.75	0.97
2	.37	.05	1.50	1.93
3	.34	.06	.90	1.25
4	.35	.06	.60	.87
5	.34	.07	.45	.74
6	.34	.06	.60	.83
7	.33	.06	.90	1.23
8	.36	.06	.90	1.34
9	.32	.07	.90	1.41
10	.37	.05	.90	1.10
11	.36	.05	1.35	1.68
12	.40	.04	1.50	1.62
13	.28	.02	2.40	.75
Average				1.21

The general expression for the law of sand transportation in the form of sand ripples remains to be obtained. As it is assumed on the basis of table 2 that in the bar environment sand transportation is independent of the position of sand ripples, the desired law can be written immediately from equation 15 with the term $\Delta H/H_1$ omitted. Accordingly,

$$\frac{Q_r T}{P_s g H_1^2} = f_2\left(P_w/P_s, \frac{\sqrt{gH_1}d_{GM}}{\nu}, \frac{H}{gT^2}, \frac{d_{GM}}{H_1}, i, \sigma_\phi\right) \tag{18}$$

In the test under study the parameters on the right hand side are constants and from the data for the test we obtain

$$\frac{Q_r T}{P_s g H_1^2} = 0.039 \tag{19}$$

The data used to establish the relation are: $Q_r = 1.21$ pounds (weight) per foot per hour, $T = 1.4$ seconds, $P_s g = 137$ pounds (weight) per cubic foot and $H_1 = 0.58$ foot. As an application to a natural condition, let us suppose that $H_1 = 6$ feet, $T = 3$ seconds and other conditions are similar to those of the test. The rate of transportation of sand would be: $Q_r = 0.039 \times 137 \times 6 \times 6/3$, or 64 pounds per foot width per hour.

The problem of sand transportation in this form of ripples on sea beds is an important one and can be treated with sufficient detail only by an independent investigation. The investigation should be made for the bar environment, and for the seaward region adjacent to the bar environment. The law probably assumes different forms in the two regions.

C. *Extreme water surface variations in the bar environment.*—The bar environment, as was mentioned previously, is limited seaward by waves which are beginning to break and shoreward by waves which reform following the breaker. Variations in the water surface elevations at these points determine the flow of energy into and out of the bar environment. In studying breaking of waves, the first question to consider is the determination of the locality where breaking is impending. The upper curve in figure 18 shows the dependence of the ratio $\Delta H_1/H_1$, upon the wave steepness, a_o/λ_0. Here H_1 is the depth of water at the locality where the waves are beginning to break, and ΔH_1 is the elevation of the crests at the point of impending wave break, measured from the level of the undisturbed water. Thus, if ΔH_1 is known the curve just given will enable us to evaluate H_1. Obviously, ΔH_1 is a function of a_o and $a_o\lambda_0$ in the form

$$\Delta H_1/a_o = f(a_o/\lambda_0) \tag{20}$$

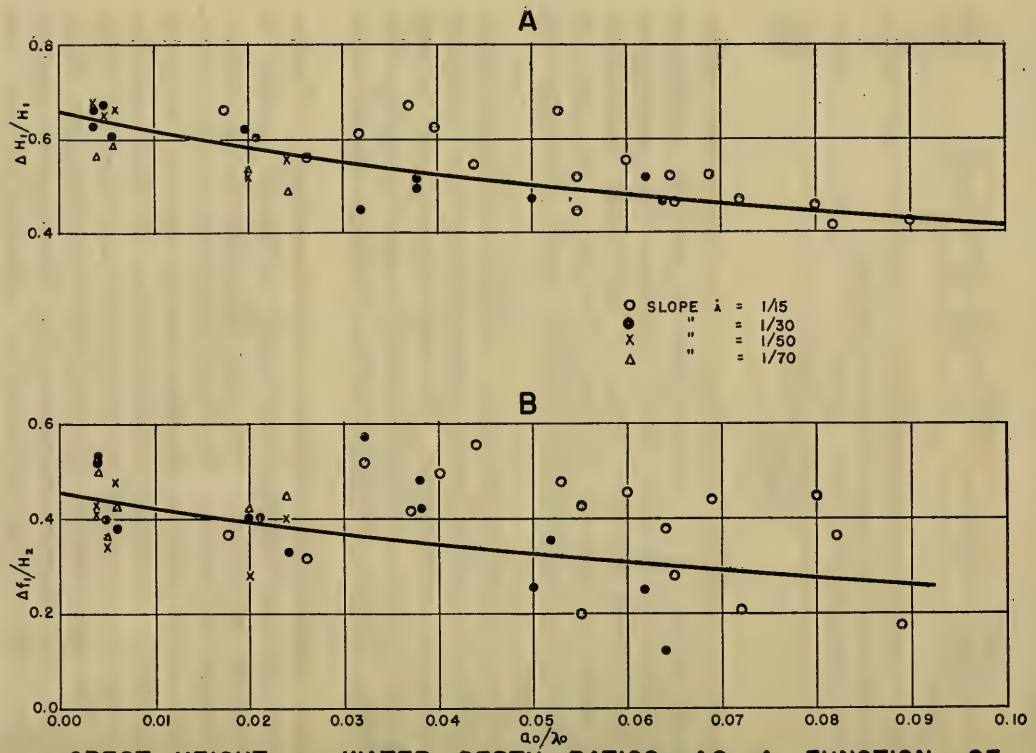

CREST HEIGHT — WATER DEPTH RATIOS AS A FUNCTION OF WAVE STEEPNESS AT START OF DEFORMATION AND RECOVERY OF WAVES

FIGURE 18.

if the effect of the slope, i, can be neglected. This relationship is shown in the upper curve of figure 19, and it is noted that the effect of slope can be neglected within the order of experimental error.

The second question to consider is the depression of the trough ΔH_2 at the start of wave break. The desired information can be obtained conveniently if we consider the ratio $\Delta H_2/\Delta H_1$ as a function of $a_o\lambda_0$. The upper curve in figure 20 approximates the relationship.

Evaluation of the energy flowing into the bar environment can be made on the basis of the quantities H_1, ΔH_1, and $\Delta H_2/\Delta H_1$. Unfortunately, the theory of shallow water waves is not complete enough for an appropriate analysis, there being available no general energy formula covering the case of breaking waves.

It is necessary to justify the absence of a_o and a_o/λ_0 in the general and transportation formulas in equations 13 and 18. It was established that $a_o/H_1=f(a_o/\lambda_0)$. By multiplying both sides of the equation by λ_0/a_o, it can be shown that there is a one to one correspondence between a_o/λ_0 and λ_0/H_1. Inasmuch as $\lambda_0=\frac{gT^2}{2\pi}$, it may be stated that a_o/λ_0 and H_1/gT^2 are uniquely related and the latter may replace the former. Because of these relations the quantities H_1 and H_1/gT^2 are sufficient to characterize, in a functional manner, the magnitude and the shape of waves entering the bar environment.

The movement of sand from the shoreward limit of the bar environment to the shore is controlled by the energy content of waves at the instant of reformation. For the evaluation of the energy the quantities H_2, Δf_1, and $\Delta f_2/\Delta f_1$ are fundamental. H_2 is the depth of water at the point where wave reformation begins, Δf_1 is the crest elevation above the undisturbed level and Δf_2 the depression of the trough below that same level. The relationship between these quantities and the wave steepness ratio a_o/λ_0 is given in figures 18, 19, and 20. These relationships should be studied further.

D. *Energy distribution in the bar environment.*—The ease with which the mathematical expressions for the form and position of bars is established results from the simplicity of the experimental procedure. The tests represent conditions under a singular system of waves and in the absence of tidal flow. Each test began with a smooth sloping surface and a bar was allowed to form and attain a relatively fixed position in association with the breaker; then, the quantities having a bearing on the form of the bar were measured. The resulting data is of the most elementary nature and really contains little information on the beach processes involved in the production of the bar. During the tests, however, attempts were made to observe these processes qualitatively.

Sand movement along the bar appears to take place in the following

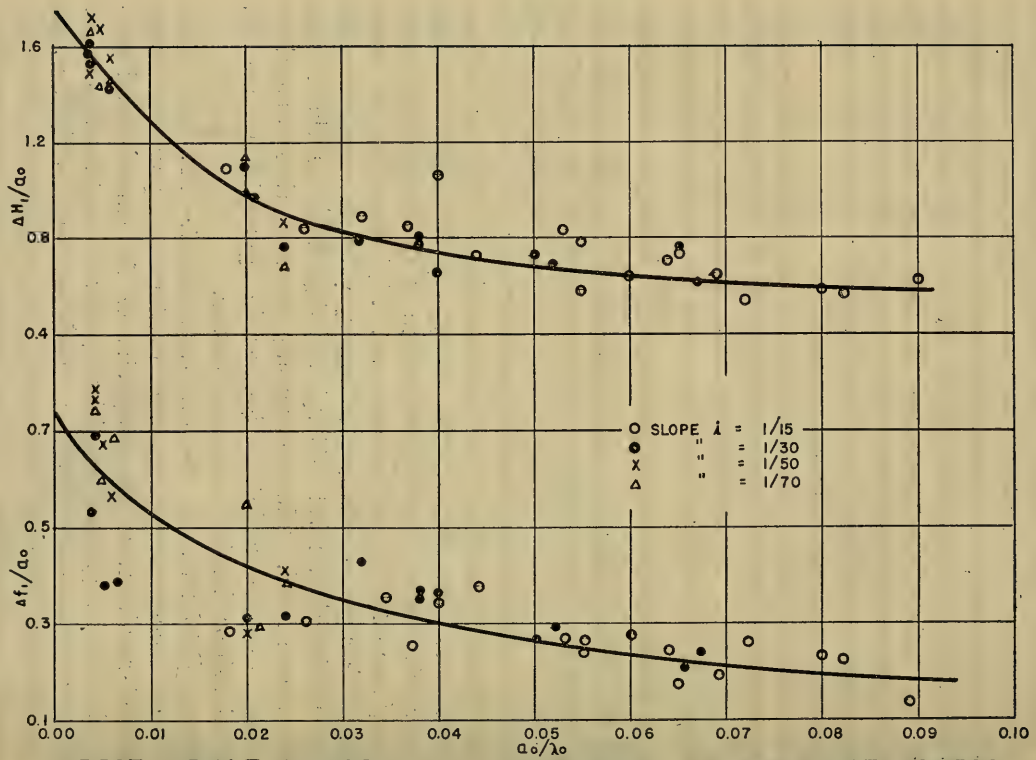

CREST HEIGHT RATIOS AS A FUNCTION OF WAVE STEEPNESS AT START OF DEFORMATION AND RECOVERY OF WAVES

FIGURE 19.

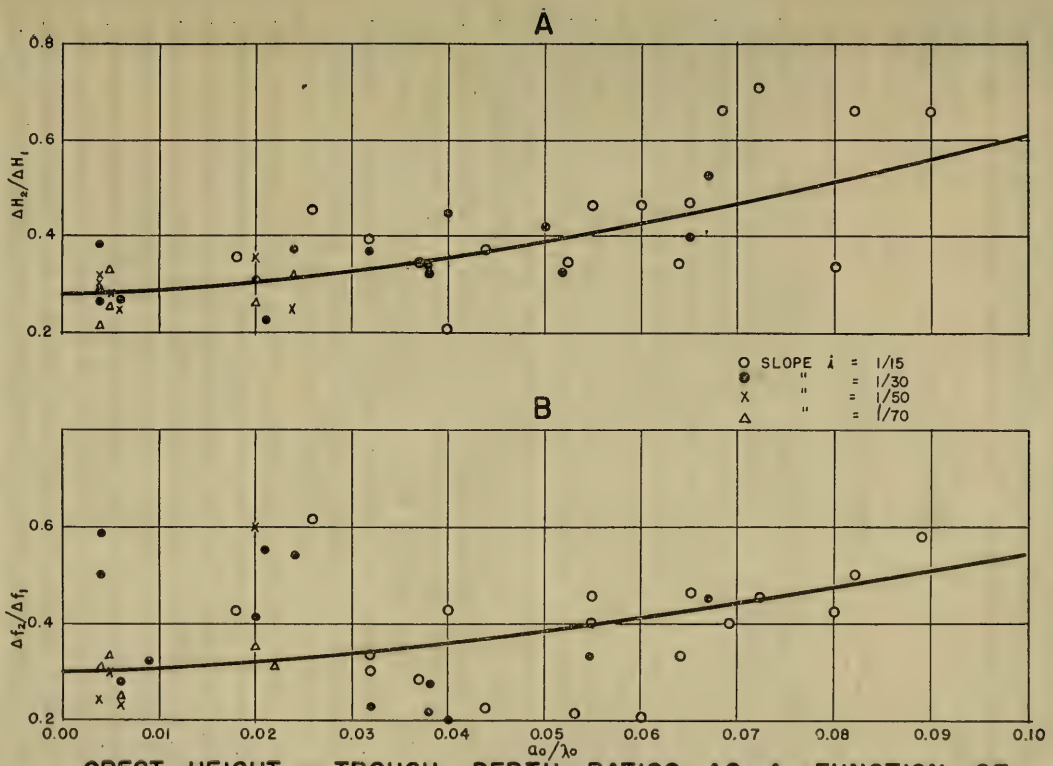

CREST HEIGHT — TROUGH DEPTH RATIOS AS A FUNCTION OF WAVE STEEPNESS AT START OF DEFORMATION AND RECOVERY OF WAVES

FIGURE 20.

manner. Initially, in the absence of the bar, a certain distance exists between the points where the wave begins to break and the breaker is completed; this distance may be referred to as the breaker distance and is denoted by s in figure 1. On flat beaches the breaker initially is of the spilling type. As the bar is formed it changes into the plunging type and the distance, s, increases. The magnitude of s is a function of the slope of the beach and of the depth of water at the point of impending wave break. The functional dependence may be expressed as

$$s/H_1 = f(a_o/\lambda_0, i) \tag{21}$$

or

$$s/H_1 = f\left(\frac{H_1}{gT^2}, i\right)$$

which probably assumes a different form when no bar is present. When bars are present, it is found that, to a rough approximation $s/H_1 = 5$, 8, 9, and 11 when $i = 1/15$, 1/30, 1/50, and 1/70, respectively.

It is the interpretation of the writer that the two changes mentioned above have a bearing on the energy distribution in the bar environment. This may be explained by reference to the two curves in figure 4 which represent the maximum and minimum elevation of the water surface with reference to the still water level during the passage of waves. In a sense these curves represent the paths of travel of the crests and troughs. In tracing the travel path of the crests, it is seen that the crest deforms rapidly and develops a central curl somewhere between the point where the wave starts to break and the plunge point. The position of the fully developed curl is shown in figure 14. The curl, or rotating body of water, causes a greater internal dissipation of energy than otherwise would be possible. After the appearance of the central curl when the water elevation is maximum at the bar crest, a strong current moves parallel to the seaward slope of the bar over the crest and is directed shoreward. The current in passing over the crest develops a curl and falls into the trough of the bar. At the instant of the fall of the curl its linear momentum is imparted to the waters ahead and the rotary momentum is consumed locally. The impact of the curl reforms the wave. In following the path of the wave troughs seaward it is seen that the current attains a maximum at the crest of the bar. The trough path at this point is a concave surface just above the seaside face of the bar, as shown in figure 14; here the hydraulic gradient is quite steep. This together with the fact that depths are small indicate the existence of a strong seaward current. The net result is that in all probability the main role of the bar is to reduce the energy of the incoming waves causing them to impart a lesser amount of energy to the reforming

waves than would be the case if the bar were absent. It is believed that the longer breaker distance signifies a greater dissipation of energy over the sand ripples as a result of increased turbulence. In such cases the rotary motions of the central curl and plunging curl are locally damped. Maximum currents over the bar are associated with loss of energy in the boundary layers over the sand.

The currents naturally affect the movement of sand in the bar environment. When the water depth over the crest is greatest the strong currents directed toward the shore move the layers of sand from that part of the seaside slope of the bar surface and the crest area into the trough of the bar. Subsequently, when the plunging curl is falling in the bar trough, the rotating water picks up sand from the trough and suspends it in the main body of water. At the instant that the depth of water over the crest is minimum, the seaward current transports the suspended sand particles and at the same time induces a movement of sand over the bar surface toward the seaside foot of the bar. In fact, the cyclic movement of sand over the bar is quite similar to that over a sand ripple, except that the advance of the main body of the bar is imperceptible. In the case of bars, the sand transported to the seaside foot of the bar by sand ripples is collected at the shore side of the bar by the recovering and reforming waves and is transported to the shore.

The formation of the main body of the bar is the final step in the sorting of sand. The coarser sand reaches the shore through the cyclic creeping movement on the surface of the sand ripples and the bar; the finer particles return to the sea through the turbulent action of the eddies of the sand ripples and the bar. This interpretation is based on incomplete data and a detailed investigation on this particular subject as an independent problem is necessary.

Section VII. ACKNOWLEDGMENT

The author acknowledges gratefully the numerous suggestions made by Dr. M. A. Mason, Chief, Engineering and Research Branch of the Beach Erosion Board, during the conduct of the tests. The importance and significance of bar structures were brought to the author's attention by Prof. W. W. Williams of Cambridge University, and his general discussions of different problems relating to the subject have been very valuable. The work of Messrs. W. H. Vesper and D. G. Dumm, who operated the models and assisted in the computations, was invaluable.

REFERENCES

1. Hagen, Gotthilf: Handbuch der Wasserbaukunst, 3 Bde. 1863.
2. Otto, Theodore: Der Darss und Zingst. Jahresber. Geogr. Ges. Greisswald, XIII, 1911–12.
3. Lehmann, F. W. Paul: Das Kustengebiet Hinterpommers. Zschr. d. Ges. f. Erdk. Berlin 19, p. 391, 1884.
4. Hartnack, Wilhelm: Uber Sandriffe, Jahresber. Geogr. Ges. Greisswald, XL–XLII, 1924.
5. Evans, O. F.: The Low and Ball of the Eastern Shore of Lake Michigan, The Journal of Geology, Vol. XLVIII, p. 476, 1940.
6. Burnside, W.: On the Modification of a Train of Waves as it advances into Shallow Water, Proc. London Math. Soc., Vol. 14, p. 131, 1915.
7. Montgomery, Lt. H. A.: Lake Michigan Wave Measurements at Milwaukee, U. S. Engineers, Milwaukee Office, Nov. 4, 1933.

U. S. GOVERNMENT PRINTING OFFICE: 1948